JOURNAL OF MATERIALS SCIENCE 25 (1990) 3814–3837

The influence of unusual counterions on the electrochemistry and physical properties of polypyrrole

K. M. CHEUNG, D. BLOOR
Department of Physics, Queen Mary College, Mile End Road, London E1 4NS, UK
G. C. STEVENS
National Power Technology and Environmental Centre, Kelvin Avenue, Leatherhead, Surrey KT22 7SE, UK

A series of different counterions have been incorporated into polypyrrole electrochemically. These include toluenesulphonate (TS), pyrenesulphonate (PSA), Pyrene-1,3,6,8-tetrasulphonate (PTSA), dodecylbenzenesulphonate (DBS), 1,2-bis(decyloxycarbonyl)ethane-1-sulphonate (DOCES), octachloro-dirhenate (Re_2Cl_8) and tetraphenylborate (TPB). Electrochemical redox behaviour of the pyrrole monomer and the polypyrrole incorporating these different anions was investigated and is discussed. From scanning electron microscopy (SEM), it is shown that the different counterions incorporated strongly affect the morphology of the polymer films, they vary from fully dense to open structures. Chemical and physical characterization of the materials is presented and suggests that the sizes of the different counterions incorporated also influence the polymer chain structures, packings and their thermal stabilities. The pyrrole to counterion stoichiometries are very different, ranging from 1 to 13. In most cases, the redox potential of the polymer can be related to the size of the counterion but the electrical conductivity, which ranges from 2×10^{-3} to $50\,S\,cm^{-1}$, is not simply related to the counterion but is dependent on both chain structure and bulk morphology.

1. Introduction

Conducting polymers are regarded as potential materials for the electronics industry especially in batteries [1], molecular transistors [2], ion-gates [3], electronic displays [4], cable shielding and as molecular electronics circuit elements [5]. Many of these are oxidised, or in some cases reduced, polymeric aromatic and heteroaromatic compounds with conductivities in a range of 10^{-1} to $10^{5}\,S\,cm^{-1}$, similar to that of semimetals and metals. Since the first observation of metallic conductivity in polyacetylene [6] and the electrochemical synthesis of free-standing polypyrrole film by Diaz *et al.* [7], the field of conducting polymers has expanded dramatically. Research has been carried out attempting to change the flexibility, solubility, electrical conductivity, mechanical properties and chemical stability of these conducting polymers. In the case of polypyrrole, the effect of different electropolymerization parameters, such as the temperature [8], the concentration of monomers and supporting electrolyte [9] with which the film was grown, the water content in the aprotic solvent [10] and the nature of the working electrodes [11, 12], have been investigated. An alternative approach has been to modify the chemical structure of the pyrrole monomers prior to electropolymerization. 3-, and 3,4-disubstituted pyrrole derivatives have been utilised, e.g. 3-alkyl [13], 3-carboxylate [14, 16], 3-cyano [17], 3-keto [18], 3-, 4-dialkyl [19] and 3-, 4-alkane-pyrrole [20, 21], etc. Besides these modifications of the electrochemical polymerization other methods have been used to prepare polypyrrole films, e.g. chemical vapour deposition (CVD) [22, 23], polymerization of LB films [24–27] and chemical preparations [28–30].

In an electrochemical preparation, the pyrrole is oxidised, forming radical cations which then dimerise and eventually the reaction proceeds to the formation of a polypyrrole film. The anions, (X^-), present in the supporting electrolyte, are incorporated in the matrix of the polypyrrole film (Fig.1), neutralizing the positive charge of the oxidized polymer. The structure of Fig. 1 is idealized and in practice there will be α–β as well as α–α bonding, crosslinks, and the ratio of chain repeat units to counterions will vary. Therefore, the anions used in the electropolymerization also play an important role in the preparation of the polypyrrole film. Many publications have reviewed the effects on polypyrrole films of incorporating different anions, e.g. long alkyl sulphate [31], Keggin-type heteropolyanions ($SiW_{12}O_{40}^{4-}$) [32, 33], phosphotungstate ($PO_4 12WO_3^{3-}$) [34], polysulphonate [35], Br, ClO_4- and AsF_6- [36, 37], etc.

In this paper we report on the physical characterization and electrochemical behaviour of polypyrrole (PPy) films containing several different anions obtained by electro-polymerized on a platinium electrode. The anions used are toluenesulphonate (TS^-), pyrenesulphonate (PSA^-), pyrene-1,3,6,8-tetrasulphonate

0022–2461/90 $03.00 + .12

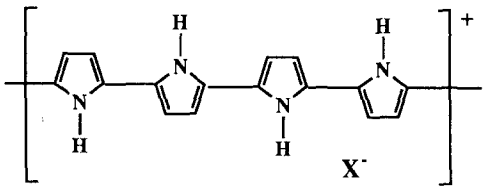

Figure 1 The structure of polypyrrole with the incorporated anion.

($PTSA^{4-}$), dodecylbenzenesulphonate (DBS^-), sodium 1, 2-bis(decyloxycarbonyl)ethane-1-sulphonate ($DOCES^-$), octachloro-dirhenate ($Re_2Cl_8^{2-}$) and tetraphenylborate (TPB^-) (Fig. 2).

The toluenesulphonate counterion has been extensively studied and it has been shown to produce polypyrrole films which are volume filling and dense with good mechanical properties, good stability and reasonable electrical conductivity (ca. 20 to 50 $S\,cm^{-1}$) [11]. It was considered important to explore the influence of other counterions with specific structural features complementary to the toluenesulphonate anion and others which could enhance chain separation and allow metallic anions to be incorporated.

The physical factors which influenced the choice of the counterions shown in Fig. 2 were:

1. PSA^- may act as a site for electron transfer (hopping) and is physically bulky;

2. $PTSA^{4-}$ can act as an electron transfer site but is bulkier, has a more regular shape and has more charges than PSA^-;

3. DBS^- has long alkyl benzene sulphonate and has surfactant properties;

4. $DOCES^-$ is similar to DBS^- but has two long flexible alkyl ester chains;

5. $Re_2Cl_8^{2-}$ is a very bulky metal containing ion and

6. TPB^- is also a very bulky ion.

These different anions should also affect the porosity, texture and redox behaviour, in particular reversibility, of the polypyrrole films.

The materials obtained were characterized by elemental analysis, resonance Raman spectroscopy, UV–visible spectroscopy, scanning electron microscopy (SEM), fast atom bombardment (FAB), thermal analysis, and d.c. electrical conductivity measurements.

2. Experimental details

2.1. Reagents

Pyrrole monomer (Aldrich) was distilled twice under reduced pressure and stored in the dark. The solvents, propylene carbonate (PC) and tetrahydrofuran (THF) (Aldrich, gold label, anhydrous) were used as supplied. Water was triply distilled and methanol was

Structure	Name	Symbol
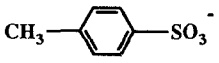	Toluenesulphonate	TS^-
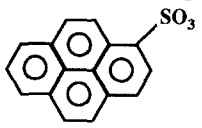	Pyrenesulphonate	PSA^-
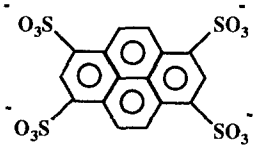	1,3,6,8-Pyrenetetra-sulphonate	$PTSA^{4-}$
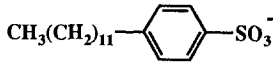	Dodecylbenzenesulphonate	DBS^-
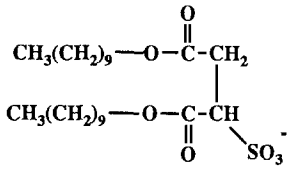	1, 2-bis (decyloxycarbonyl)-ethane-1-sulphonate	$DOCES^-$
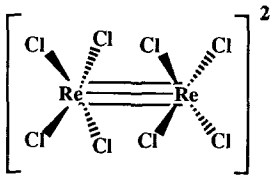	Octachlorodirhenate	$Re_2Cl_8^{2-}$
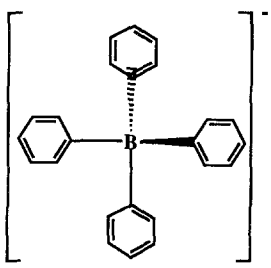	Tetraphenylborate	TPB^-

Figure 2 The structures, names and symbols of the anions used to incorporate in the polypyrrole.

dried and distilled. The supporting electrolytes, lithium perchlorate ($LiClO_4$), tetrabutylammonium octachlorodirhenate ($2TBA^+ Re_2Cl_8^=$), tetrabutylammonium tetraphenylborate (TBA^+TPB^-) (Aldrich) and 1,3,6,8-pyrenetetrasulphonic acid tetrasodium salt ($4Na^+PTSA^{4-}$) (Kodak) were used as supplied. Tetraethylammonium p-toluenesulphonate (TEA^+TS^-) was dried by heating at 100° C for 24 h *in vacuo*. Tetraethylammonium dodecylbenzene-sulphonate (TEA^+DBS^-), tetraethylammonium pyrene-sulphonate TEA^+PSA^- and sodium 1,2-bis(decyloxycarbonyl) ethane (Na^+DOCES^-) were prepared as follows.

2.2. Synthesis of TEA^+PSA^-

Pyrenesulphonic acid [38] (6 g, 2.13×10^{-2} mol) was dissolved in water (20 ml), resulting in a silky green solution. Tetraethylammonium hydroxide (40%) (7.83 g, 2.2×10^{-2} mol) was then added, and the resultant brown solution heated up to ca. 50° C and stirred for 10 h. The water was evaporated off and a greenish-brown syrup, which solidified when left in air for a few hours was obtained. The solid was then dissolved in $CHCl_3$ (80 ml) and filtered. After evaporation of the solvent, a brown solid was obtained (5.3 g, 58% yield).

2.3. Synthesis of TEA^+DBS^-

Dodecylbenzenesulphonic acid (44.3 g, 1.36×10^{-1} mol) (donated by Tenneco Co., Albright & Wilson Ltd., detergent division) was neutralized by an equimolar amount of tetraethylammonium hydroxide (40%) (50 g, 1.36×10^{-1} mol). The procedure for the preparation of TEA^+DBS^- was similar to that for the preparation of TEA^+PSA^-. The resulting semi-solid was dissolved in $CHCl_3$ (200 ml) and filtered. After evaporation of the solvent, a light yellow semi-solid was obtained (38 g, 59.1% yield).

2.4. Synthesis of Na^+ 1,2-bis(decyloxycarbonyl)ethane-1-sulphonate [39]

Maleic acid (16.6 g, $1.43 \times 10^-$ mol) was dissolved in acetone (150 ml) and decanol (45.2 g, $2.86 \times 10^-$ mol) and 5 drops of concentrated H_2SO_4 were added. The mixture was refluxed overnight, resulting in a red solution. After evaporation of the solvent, $NaHCO_3$ solution was added, and a foamy, milky suspension was obtained. The ester was then extracted with CH_2Cl_2 (2×200 ml), washed with NaCl solution (1×300 ml) and dried in a Na_2SO_4. After evaporation of the solvent, a yellow liquid (18 g, 31% yield) was obtained.

The ester (18 g, 7.56×10^{-2} mol) was mixed with $CHCl_3$ (20 ml) and a solution of $Na_2S_2O_5$ (5.5 g, 2.89×10^{-2} mol) was added. The mixture was refluxed for 2 days and filtered. After addition of 500 ml hot methanol and cool down, the methanol was then removed by evaporation until a white powder was observed in the solution, at which point, the solution was cooled in ice. The solid was then filtered off and dried, yielding a white powder (6 g, 23.2%).

All these salts gave elemental analysis, NMR and IR spectra consistent with the chemical formulae.

2.5. Electrochemical methods

Electropolymerization was carried out under galvanostatic control using a Thompson Electrochem 401 potentiostat in a single compartment cell under nitrogen. Two $35 \times 35\,mm^2$ platinum titanium electrodes (ICI Electrochem Co.) with a separation of ca. 40 mm were used.

Cyclic voltammetry (CV) of the pyrrole monomer and the polypyrrole films was carried out in a 100 ml glass cell with a fitted cork stopper which held a saturated calomel reference electrode (SCE), platinum working eletrode (disc, dia. = 3 mm) and a platinum counter electrode (disc, dia. = 1 mm). The CV experiments were run using an in-house potentiostat with a built-in sweep generator, and the voltammograms were recorded on a Bryans 5000 *XY* recorder.

A typical pyrrole/electrolyte composition was ca. 6.0×10^{-3} M pyrrole and 0.1 M TEAX/PC, where TEA is tetraethylammonium and X is the corresponding anion. When X was $Re_2Cl_8^=$ and $DOCES^-$, concentrations of TEAX were 0.01 M and 0.04 M, respectively. All the solutions were flushed with nitrogen before each experiment. Various amounts of charge in the range 800–1000 C were passed at a current density of 0.82 $mAcm^{-2}$ to produce film thicknesses from 0.2 to 0.4 mm. After each polymerization, the films were peeled off the electrode and washed in water and acetone in an ultrasonic bath three times before being dried without heating *in vacuo*. In the case of PPy/Re_2Cl_8, the film was washed in water and acetone in an ultrasonic bath first before being peeled off the electrode. For PPy/PSA, the polymer which was powdery, was washed in water and acetone before being scraped off the electrode for analysis. For CV, different quantities of pyrrole monomer were used (3.13×10^{-2} mol dm^{-3} for PPy/TS, 1.15×10^{-1} mol dm^{-3} for PPy/PSA, 1.15×10^{-1} mol dm^{-3} for PPy/PTSA, 4.48×10^{-2} mol dm^{-3} for PPy/DBS, 1.49×10^{-3} mol dm^{-3} for PPy/DOCES, 8.36×10^{-2} mol dm^{-3} for PPy/Re_2Cl_8) and background scans of the pure electrolyte were also recorded.

2.6. Chemical and physical characterization

Elemental analysis (EA) of C, H, N, S, O was carried out by the University of London analysis service at University College and EA of Re and Cl at the Chemistry Department of Brunel University. Resonance Raman spectroscopy was employed as described elsewhere [11]. UV absorption spectra were recorded on a Perkin-Elmer 555 spectrophotometer. Differential scanning calorimetry (DSC) and thermogravimetric analysis (TGA) was carried out on a Perkin Elmer 7 series system. Scanning electron microscopy was performed on a Hitachi S800 microscope employing a field emission source.

In the fast atom bombardment (FAB) experiment, the source and the fast atom gun was manufactured by M-Scan Co. The Argon atoms were accelerated at about 6 kV and the fragment signals were recorded on a Kratos MS 50RF mass spectrometer.

X-ray diffraction patterns were recorded on a Philips diffractometer comprising a PW 1743 generator control, PW 1390 channel control, PW 1394

(a) pyrrole / TEA-TS / PC

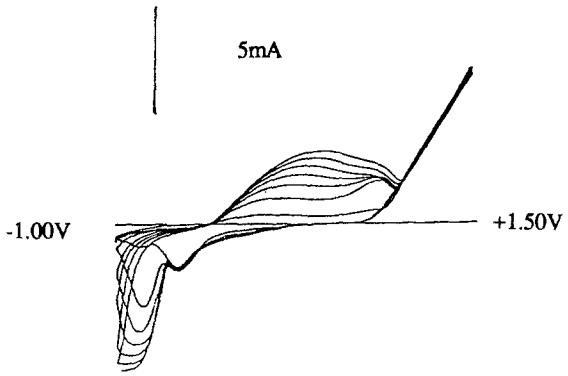

Figure 3 Cyclic voltammograms of pyrrole; scan speed = 50 mV sec^{-1}; of concentrations (a) 3.13×10^{-2} mol dm^{-3} in 0.1 M TEA-TS/PC, (b) 1.15×10^{-1} mol dm^{-3} in 0.1 M TEA-PSA/PC, (c) 1.15×10^{-1} mol dm^{-3} in 0.1 M TEA-PSA (1% H_2O)/PC, (d) 1.15×10^{-1} mol dm^{-3} in 0.1 M 4Na-PTSA/H_2O, (e) 4.48×10^{-2} mol dm^{-3} in 0.1 M TEA-DBS/PC, (f) 1.49×10^{-2} mol dm^{-3} in 0.04 M Na-DOCES/MeOH, (g) 8.36×10^{-2} mol dm^{-3} in 0.01 M 2TBA-Re_2Cl_8/PC.

(b) pyrrole / TEA-PSA / PC

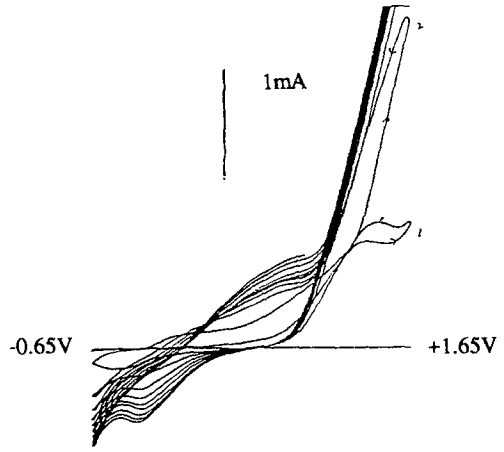

(c) pyrrole / TEA-PSA-1%H_2O / PC

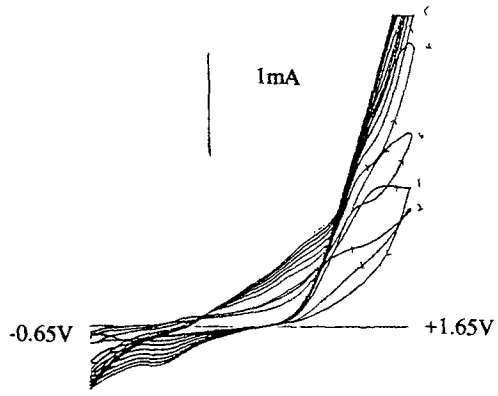

(d) pyrrole / PTSA-4Na / H_2O

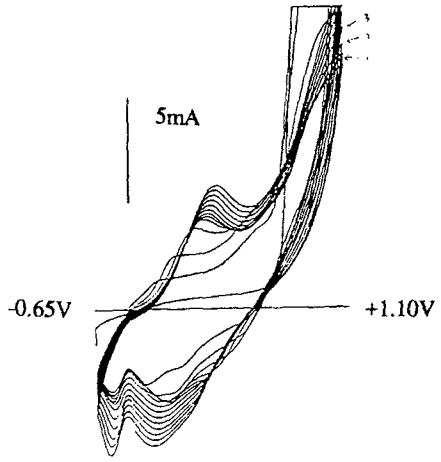

(e) pyrrole / TEA-DBS / PC

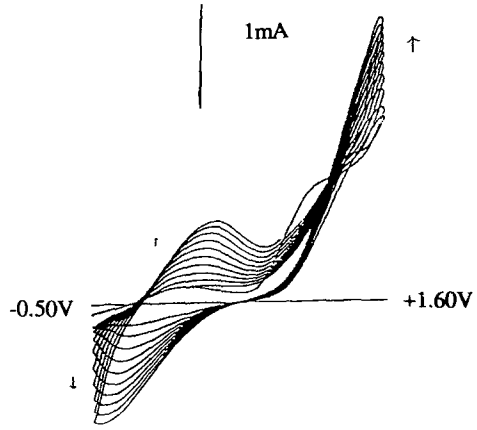

(f) pyrrole / DOCES-Na / MeOH

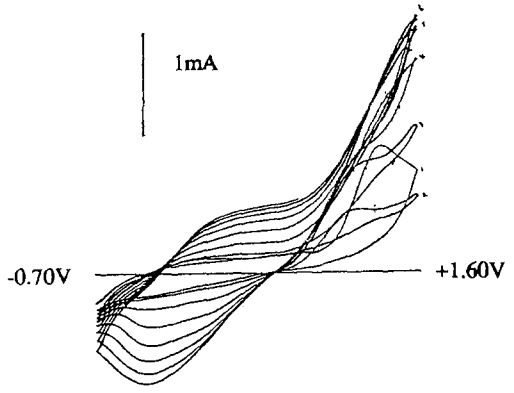

(g) pyrrole / 2TBA-Re_2Cl_8 / PC

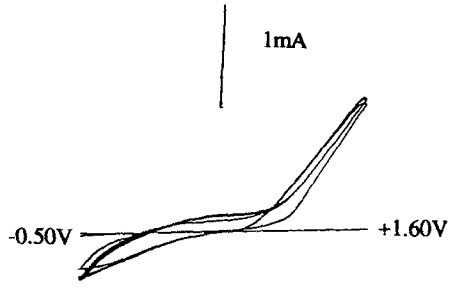

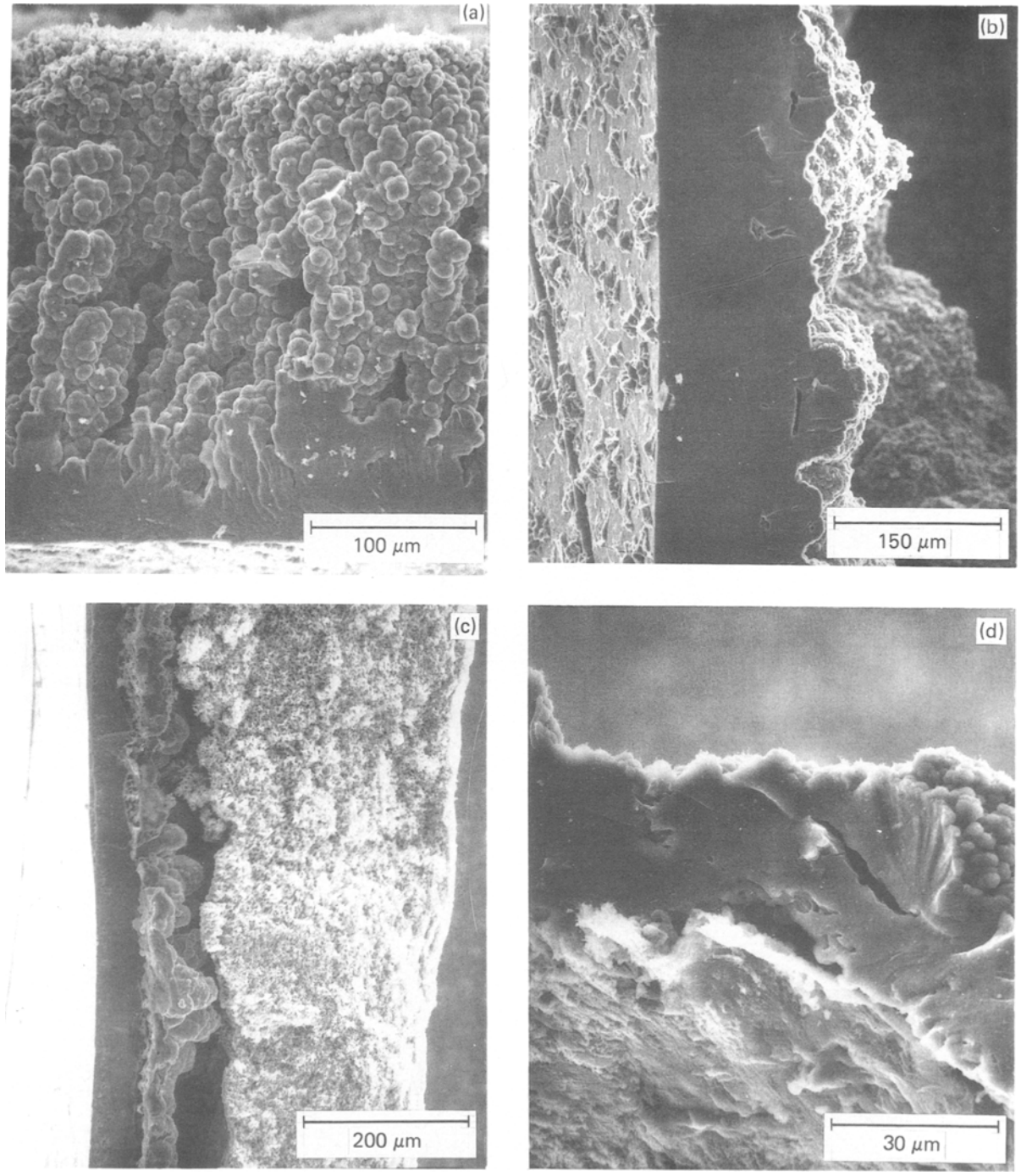

Figure 4 SEM micrographs of polypyrrole film fracture surfaces illustrating the through-film morphology. (a) PSA^-, (b) $PTSA^{4-}$, (c) DBS^-, (d) $DOCES^-$ and (e) $Re_2Cl_8^{2-}$.

motor control, PM 8203 chart recorder and PW 1050/25 goniometer. The Cu$K\alpha$ radiation was employed with the tube operated at a voltage of 50 kV, and a current of 30 mA.

2.7. Monomer oxidation and electropolymerization

The oxidation peak of the pyrrole monomer was observed with varying degrees of clarity in these electrolyte solutions. Clear definition of the peak occurred in the cases of TEA-PSA/PC, TEA-PSA (1%H_2O)/PC, TEA-DBS/PC and Na-DOCES/MeOH (Fig. 3b, c, e and f). In all cases, the peak current and shape of the second and subsequent scans were different from those of the first scan. This implies that the mechanism of the formation of the film produced during the first cycle is different from that of subsequently polymerized layers. This was supported by earlier SEM observations on the TS^- anion system where a region immediately adjacent to the metal electrode surface was found which was morphologically different to the remainder of the polymer [11].

This morphological distinction is even more pronounced for the polypyrrole materials investigated here as shown in the micrographs in Fig. 4. In the case of the $Re_2Cl_8^{2-}$, PSA^- and DBS^- anions (Figs. 4e, a and c), clearly defined dense layers exist at the electrode interface ranging in thickness from about 10, 25 and 50 μm respectively. The film morphology then progresses through a gradation of globular and par-

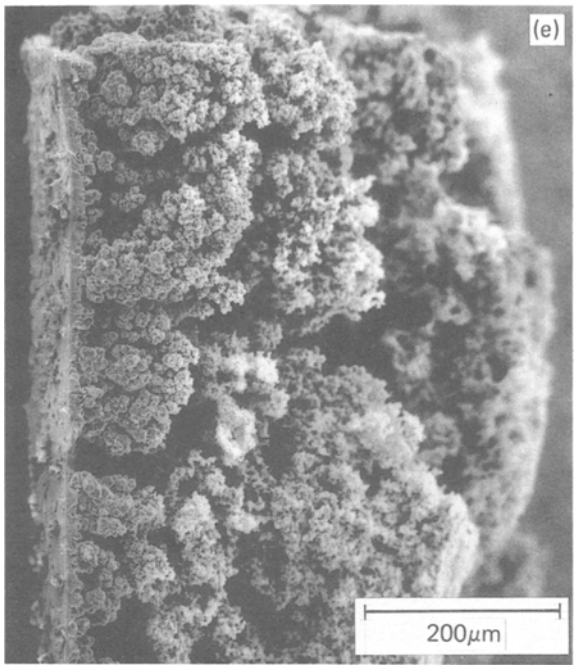

Figure 4 Continued.

ticulate aggregates to form open surface structures in contact with the electrolyte. Typical electrolyte contacting surfaces are shown in Fig. 5. In all cases the size range of the smallest particulates is 0.2 to 1 μm.

The $PTSA^{4-}$ and $DOCES^{-}$ materials appear to be as fully dense as TS^{-}. However, in contrast to TS^{-} they contain a high level of internal voiding in spite of having close packed electrolyte surfaces as shown in Fig. 5. Also, in the $DOCES^{-}$ case, detachment of a thin layer in contact with the electrode was observed indicative of the presence of a layer structure. No layer structure was observed in PPy/PTSA samples.

Generally, the peak current of the pyrrole monomer increased when the scans were performed sequentially (see Fig. 3). In the Na-PTSA/H_2O electrolyte system (Fig. 3d), the oxidation peak current dropped gradually and then increased again. An extra peak was observed with a cathodic potential (E_p^c) of -0.60 V. This was not a reduction peak of the polypyrrole film, which was being formed, since no such peak was observed when the CV of the polymers, PPy/PTSA, was run in a clean electrolyte solution (see Fig. 8f and g). This extra peak was probably due to the reduction of a small number of accumulated protons which remained in the vicinity of the working electrode instead of migrating to the counter electrode.

When pyrrole monomer was oxidised in the 2TBA-Re_2Cl_8/PC electrolyte system (Fig. 3g), the CV was ill defined. In spite of this, a good film was produced both in a direct electropolymerization and in CV experiments. In a control experiment, it was found that the supporting electrolyte, $2TBA^{+}Re_2Cl_8^{=}$ was itself electroactive at the potential required to oxidise the pyrrole monomer. It was therefore assumed that both the $2TBA^{+}Re_2Cl_8^{=}$ and the pyrrole monomer were oxidized simultaneously during the electropolymerization.

The $Re_2Cl_8^{=}$ ion showed two oxidation and one reduction peaks, $E_p^a(1) = +1.20$ V, $E_p^a(2) = +1.82$ V; $E_p^c(1) = +0.40$ V (against SCE) at the first cycle in the range 0 to 2.3 V. A new oxidation peak was obtained at the second cycle at $+0.70$ V (Fig. 6a). When the scan was repeated, the first oxidation peak shifted and deformed, finally, a peak at $+1.65$ V was obtained. A possible explanation for this behaviour is that after $Re_2Cl_8^{=}$ is oxidized to form $Re_2Cl_8^{-}$ at the first oxidation potential, it has two reaction pathways, (a) dimerization to form $(Re_2Cl_8)_2^{=}$; (b) dissociation to form $Re_2Cl_7^{-}$ and Cl^{-}.

The second oxidation potential represents the oxidation of the dimer $(Re_2Cl_8)_2^{=}$ to form $(Re_2Cl_8)_2^{-}$ and eventually polymeric ions will be obtained. The reduc-

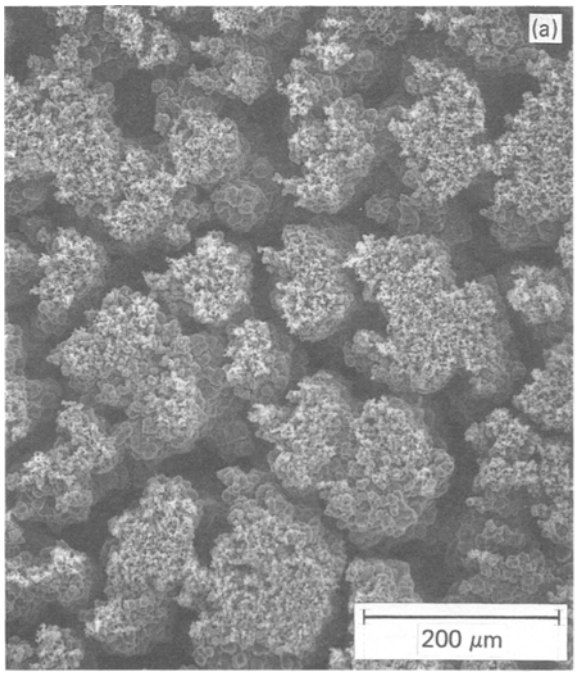

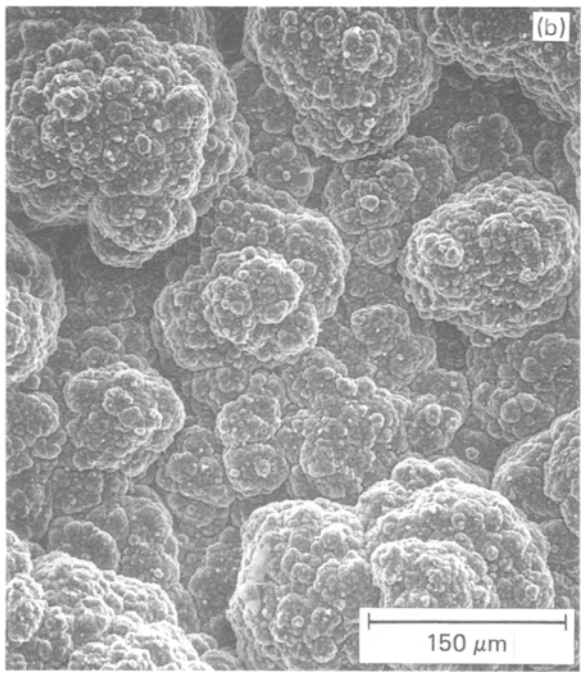

Figure 5 SEM micrographs of the electrolyte facing surfaces of polypyrrole films. (a) PSA^{-}, (b) $PTSA^{4-}$, (c) DBS^{-}, (d) $DOCES^{-}$ and (e) $Re_2Cl_8^{2-}$.

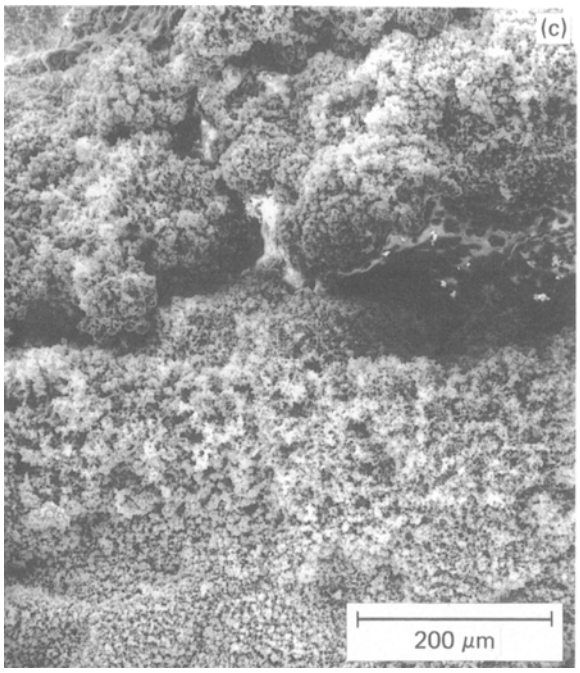

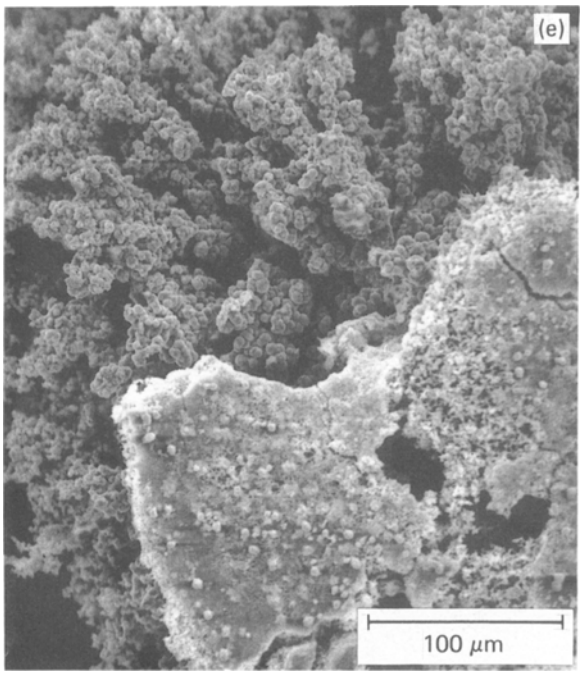

Figure 5 Continued.

tion potential at +0.40 V represents the reduction of $Re_2Cl_7^-$ after the dissociation to form $Re_2Cl_7^-$ which then reoxidizes at +0.70 V during the second cycle. The polymeric ions are probably "passivating" and interfere with the oxidation of $Re_2Cl_8^=$ during the second and subsequent cycles. It can be seen in Fig. 6b, that when the scan was in the range 0 to 1.50 V, i.e. eliminating the chance of polymerization to $(Re_2Cl_8)_n^=$, the current density of the first oxidation peak did not shift and deform. Comparing the current densities, it can be said that the dimerization of $Re_2Cl_8^-$ was more rapid than the dissociation. The proposed mechanism is summarized in Fig. 7.

Therefore, during the controlled current electropolymerization, the major anion incorporated in the polypyrrole film is likely to be the dimeric ion, $(Re_2Cl_8)_2^{2-}$ but the presence of the polymeric form cannot be excluded.

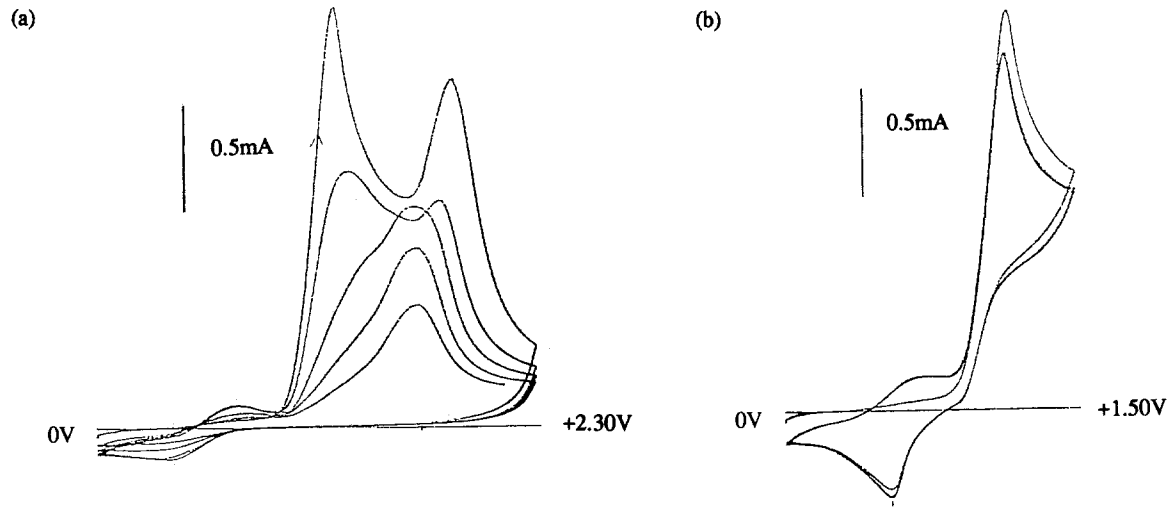

Figure 6 CV of $2TBA^+ Re_2Cl_8^=$ in 0.1 M TEA-TS/PC (against SCE); scan speed = 50 mV sec^{-1}, (a) from 0 to 2.3 V, (b) from 0 to 1.5 V.

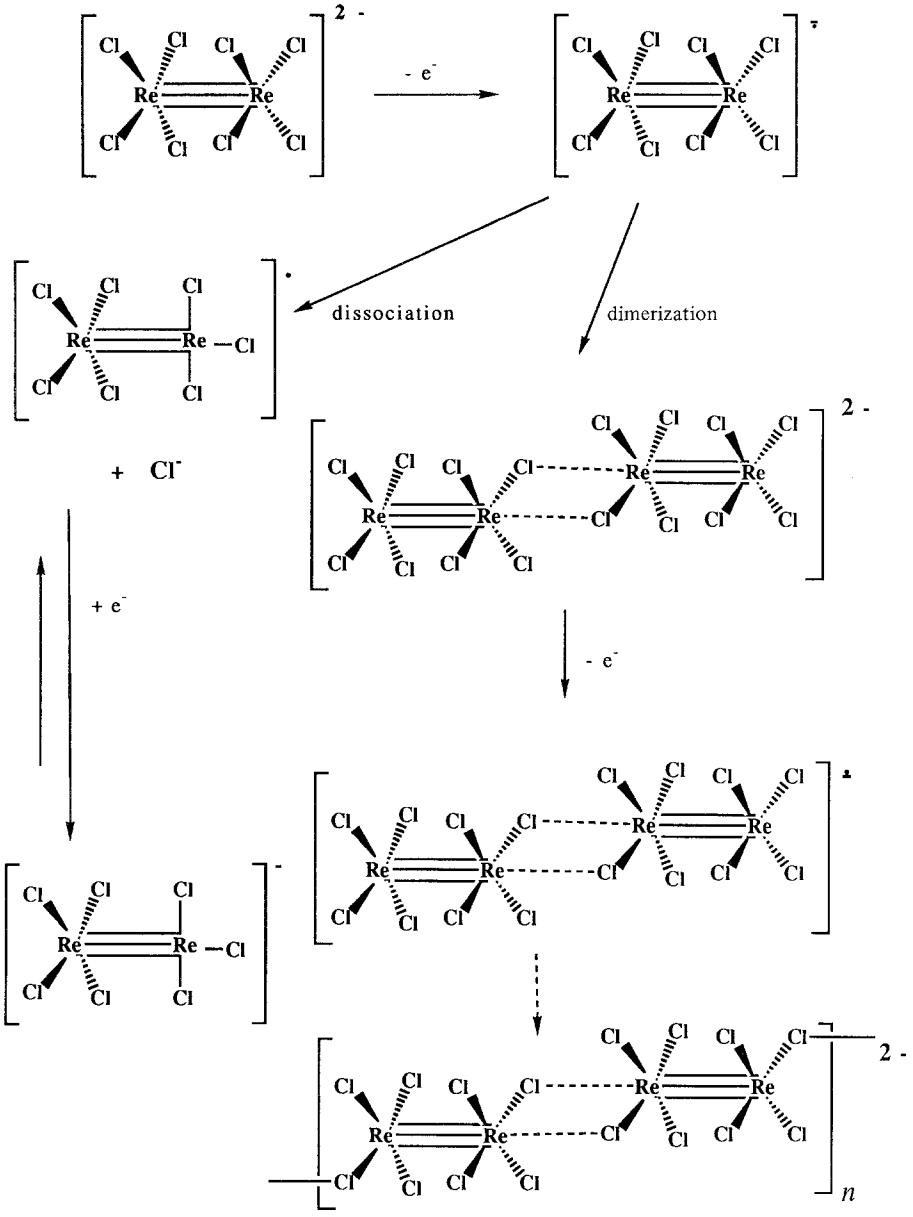

Figure 7 The proposed electrochemical mechanism of octochlorodirhenate anion.

In X-ray diffraction experiments, amongst all of the polypyrrole samples, only PPy/Re_2Cl_8 showed an ordered structure. Only one strong diffraction peak was obtained which indicated a layer spacing of about 3 nm. The absence of weaker diffraction peaks suggests that a superlattice structure may be formed resulting from intercalation of the octochlorodirhenate and the polypyrrole. Such intercalation has been proposed in the PPy-FeOCl system with the production of a 26 nm layer spacing [40, 41].

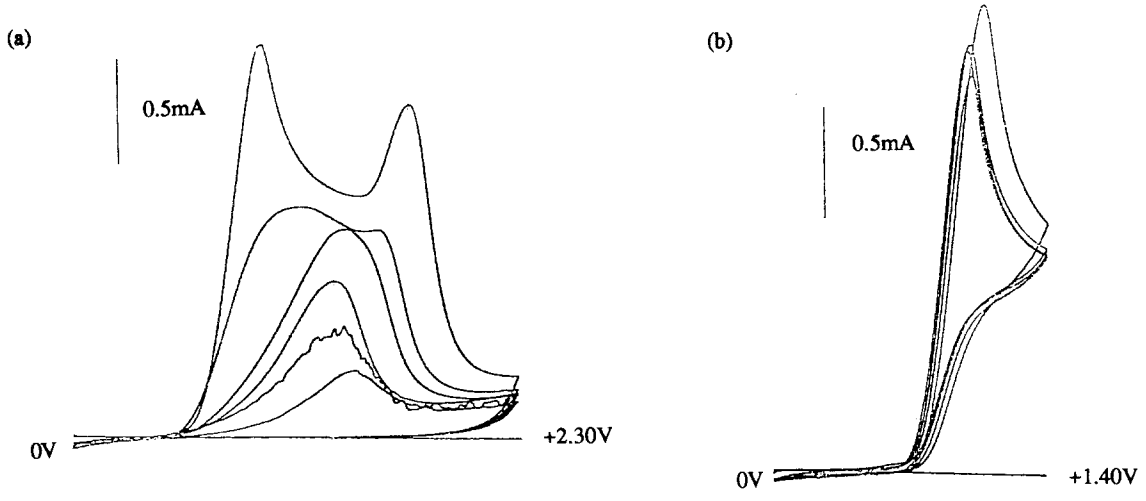

Figure 8 CV of TBA^+TBP^- in 0.1 M TEA-TS/PC (against SCE); scan speed = 50 mV sec^{-1}, (a) from 0 to 2.3 V, (b) from 0 to 1.4 V.

When pyrrole was oxidized in the TBA-TPB/PC electrolyte system, the usual black polymer film was not obtained. It was found that the TPB^- ion has a lower oxidation potential than the pyrrole monomer, hence during the electropolymerization, the oxidation of TPB^- ion was preferred. The TPB^- ion shows two oxidation peaks (Fig. 8a). The first peak represents the oxidation of the TPB^- ion to $TPB^{\cdot}$ radical which dissociated rapidly to produce triphenylborate and a phenyl radical. The phenyl radical dimerised rapidly to form biphenyl which was oxidised at the second oxidation peak to form polyphenylene(lit. E_p^a of biphenyl was +1.90 V against SCE, CH_3CN, Pt electrode [42]). The mechanism for this reaction is proposed in Fig. 9 and was verified by a controlled potential electrolysis. TBA^+TPB^- (0.34 g, 7.58×10^{-4} mol) was oxidized at +0.94 V in 0.1 M TEA-TS/PC (against SCE). After the charge consumption was about equivalent to 1 F mol^{-1}, the product was isolated. Biphenyl (0.06 g, 51.4% yield) was obtained, the m.p. was 70–71° C (lit. m.p. = 69–72° C [43]).

As can be seen from Fig. 8b, the repeated oxidation of the TPB^- proceeded normally when the scan was from 0 to 1.5 V. When, however, the scan range was from 0 to 2.3 V (Fig. 8a), the oxidation peak of TPB^- was shifted to a more anodic value and deformed. This was due to the interference of the polyphenylene film being formed at +1.70 V. Since polyphenylene is not a good conducting polymer when prepared in neutral solution [44], it acts as a passivating layer on the electrode. This explains why the current densities of the second and the consecutive oxidation peaks of TPB^- decreased, and why the oxidation peaks became more anodic.

In the cases of TEA-DBS/PC (Fig. 3c), Na-DOCES/MeOH (Fig. 3f), TEA-PSA/PC (Fig. 3b) and TEA-PSA (1% H_2O)/PC (Fig. 3c), the current on the reverse sweep is higher than the forward one. This is a common observation where a surface phase is formed by a nucleation and growth mechanism [45]. Usually, the oxidation potential of the second scan is higher than that of the first, but the current density is less. This suggests that the oxidation of the pyrrole monomer is more difficult on the first layer of the "polypyrrole" electrode. On the third and consecutive scans, the current increases again. This suggests that there may be a "catalysis-via-mediator" effect (in which the polypyrrole film acts as a mediator) [46] (Fig. 10) on the oxidation of the pyrrole monomer when the reasonably thick polypyrrole acts as an electrode.

2.8. CV of polymer

The redox behaviour of polypyrroles with different

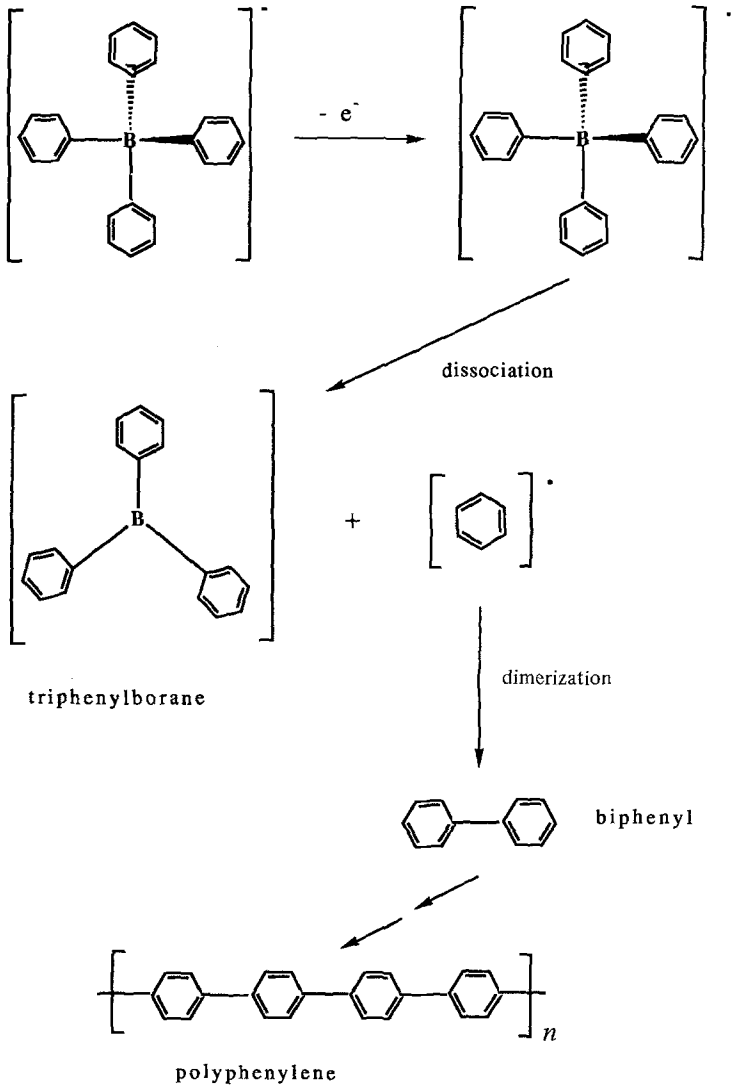

Figure 9 The proposed oxidation mechanism of tetraphenylborate anion.

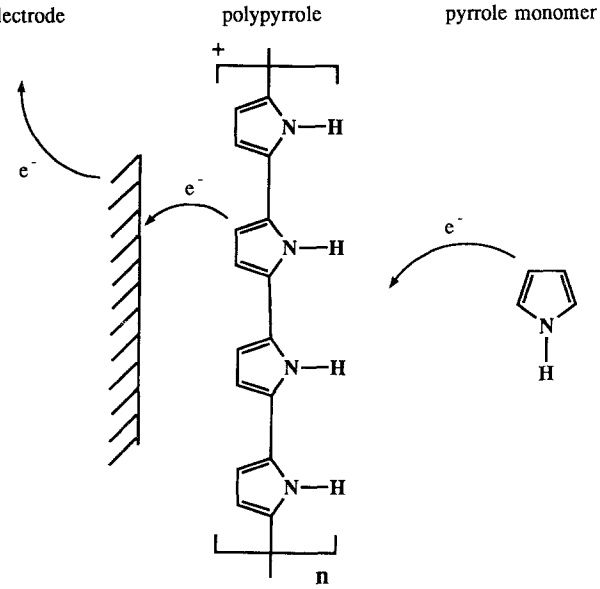

Figure 10 The proposed mechanism of 'catalysis-via-mediator'.

incorporated anions were studied in two clean supporting electrolyte/solvent systems, namely, TEA-TS/PC and TEA-X/PC where X represents the corresponding incorporated anion. Generally, the polypyrroles in TEA-TS/PC have better well-defined cyclic voltammograms (Fig. 11).

The redox behaviour of polypyrrole during cyclic voltammetry is divided into three distinct stages (Fig. 12). Firstly, during the first half-cycle when the polymer is run, say from -0.5 to $+0.5$ V, it is driven into the neutral state, i.e. all the anions have already been expelled (see Fig.13a). Secondly, when the potential reaches the corresponding oxidation potential of the neutral polymer, the polymer is oxidized and the anions diffuse back into the polymer to maintain charge neutrality (see Fig. 13b). Thirdly, when the scan is cycled back, at the corresponding reduction potential of the polymer, it is reduced and the anions are expelled again (see Fig. 13c).

Table I shows the redox potentials of polymer films with different anions incorporated. When we compare the redox potentials of the polypyrrole with the same anion in the two electrolyte/solvent systems, the difference is not great, e.g. comparing PPy(PSA)/TEA-PSA/PC and PPy(PSA)TEA-TS/PC systems, $\Delta E_p^a = 0.03$ V. It suggests that the redox behaviour of polypyrrole is independent of the electrolyte/solvent system. But in the case of PPy/Re_2Cl_8, it behaves differently, ΔE_p^a is 0.17 V. This is probably due to the large size of the $(Re_2Cl_8)_2^{2-}$ ion in comparison with the TS^- ion. During polymerization the inclusion of the large and rigid ions such as $PTSA^{4-}$ and $Re_2Cl_8^{2-}$ will lead to them occupying a relatively large volume fraction resulting in a bulk polymer structure which is potentially more porous than that resulting from the inclusion of smaller and more flexible anions such as TS^- and $DOCES^-$. If this is the case the polypyrroles formed with the larger and more rigid anions would favour oxidation potentials which are less anodic and reduction potentials which are less cathodic compared with PPy/TS; this is indeed the case. This increased bulk porosity should not be confused with the presence of a more or less densely packed film structure (c.f. $PTSA^{4-}$ Figs 4b and 5b and $Re_2Cl_8^{2-}$ Figs 4e and 5e). DBS^- and $DOCES^-$ anions are also large but flexible, therefore, although the oxidation potential is less anodic and the reduction potential is less cathodic, the magnitude is not as great as in the cases of $PTSA^{4-}$ and $Re_2Cl_8^{2-}$ ions.

Whilst increased polymer porosity explains the PPy/Re_2Cl_8 observation it is also possible that chain perfection may contribute to the differences observed in the redox potentials. Indeed, since a polymer with more extensive conjugation exhibits a lower oxidation potential (c.f. [47], in which E_p^a of cyclohexene is 2.14 V whereas E_p^a of 1,4-cyclohexadiene is 1.74 V, against SCE, in 0.1 M $LiClO_4/CH_3CN$, using a platinum electrode), it is possible that the larger anions produce a more regular chain structure with a higher degree of conjugation. So, both chain packing and chain perfection are probably related to the anion used.

In the same table, we can see there is a significant difference of about 0.21 V between the oxidation poten-

TABLE I The redox potentials and peak separations of PPy films with different anions incorporated.

Counter-ion incorporated in PPy/electrolyte (solvent)* in which PPy CV was taken	Redox potential† E_p^a/E_p^c (V)	Peak separation (V)
TS/TEA-TS (PC)	+0.40/−0.69	1.09
PSA/TEA-PSA (PC)	+0.47/−0.53	1.00
PSA/TEA-TS (PC)	+0.50/−0.51	1.01
PSA‡/TEA-PSA (PC)	+0.26/−0.31	0.57
PSA‡/TEA-TS (PC)	+0.30/−0.27	0.57
PTSA/$LiClO_4$ (H_2O)	−0.23/−0.50	0.27
PTSA/TEA-TS (PC)	−0.17/−0.34	0.27
DBS/TEA-DBS (PC)	+0.21/−0.25	0.46
DBS/TEA-TS (PC)	+0.18/−0.17	0.35
DOCES/Na-DOCES (MeOH)§	−/−	–
DOCES/TEA-TS (PC)	+0.10/−0.33	0.43
Re_2Cl_8/2TBA$^+$ $Re_2Cl_8^=$ (PC)‖	+0.19/−0.53	0.72
Re_2Cl_8/TEA-TS (PC)	+0.02/−0.32	0.34

*The concentration of electrolyte (solvent) was about 0.1 M.
† Ref. electrode was SCE; the potentials were measured at scan speed = 50 mV sec^{-1}.
‡ The PPy was prepared in the presence of 1% H_2O.
§ The concentration of electrolye (solvent) was about 0.04 M.
‖ The concentration of electrolyte (solvent) was about 0.01 M.
–Not well defined.

(a) PP (TS) / TEA-TS / PC

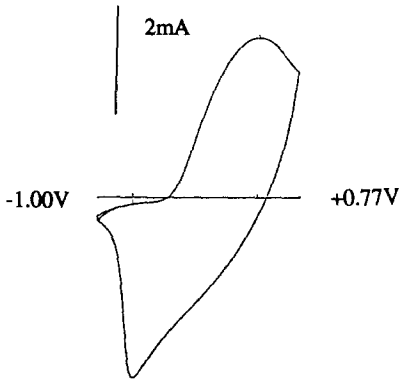

tials of PPy/PSA (+0.47 V) and PPy/PSA (1%H_2O) (+0.26 V). It suggests that water in some way also affects the conjugated chain structures.

Due to the complication of the capacitive current in the cyclic voltammograms, the reversibility cannot be defined by using Nernst's Equation which states that $(E_p^a - E_p^c) = 0.059$ V. Therefore, the reversibility of these polymers can only be estimated by measuring the i_p^a/i_p^c ratios. Table II shows that the i_p^a/i_p^c ratios of the various polypyrroles, are close to unity.

Figure 11 CVs of polypyrrole with different anions in various supporting electrolyte/solvent systems.

(b) PP (PSA) / TEA-PSA / PC

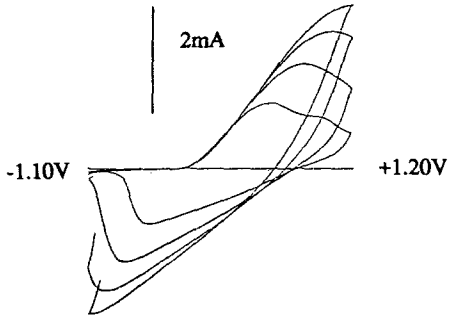

(c) PP (PSA) / TEA-TS / PC

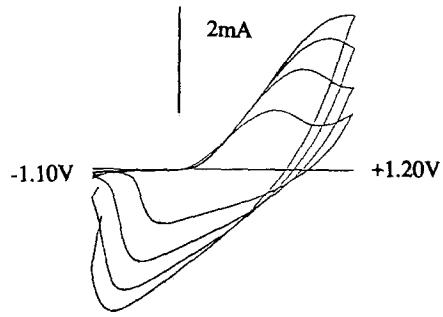

(d) PP (PSA-1% H_2O) / TEA-PSA /PC

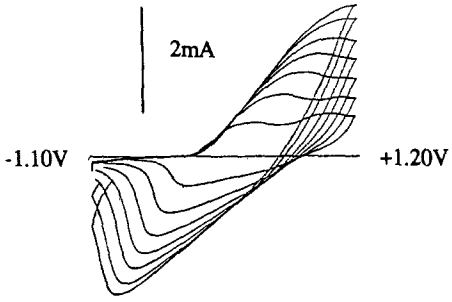

(e) PP (PSA-1% H_2O) / TEA-TS / PC

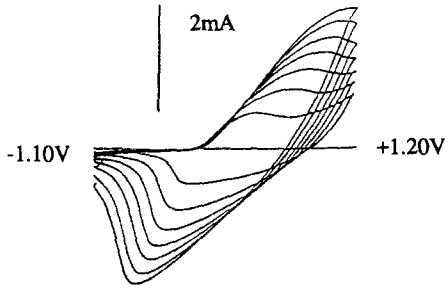

(f) PP (PTSA) / $LiClO_4$ / H_2O

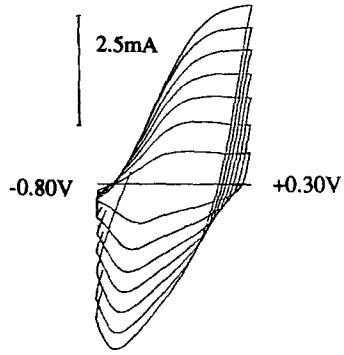

(g) PP (PTSA) / TEA-TS / PC

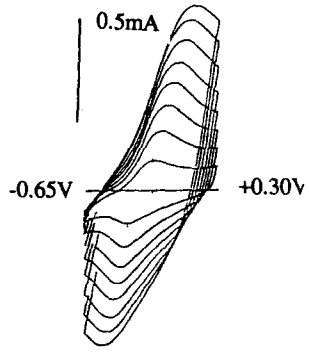

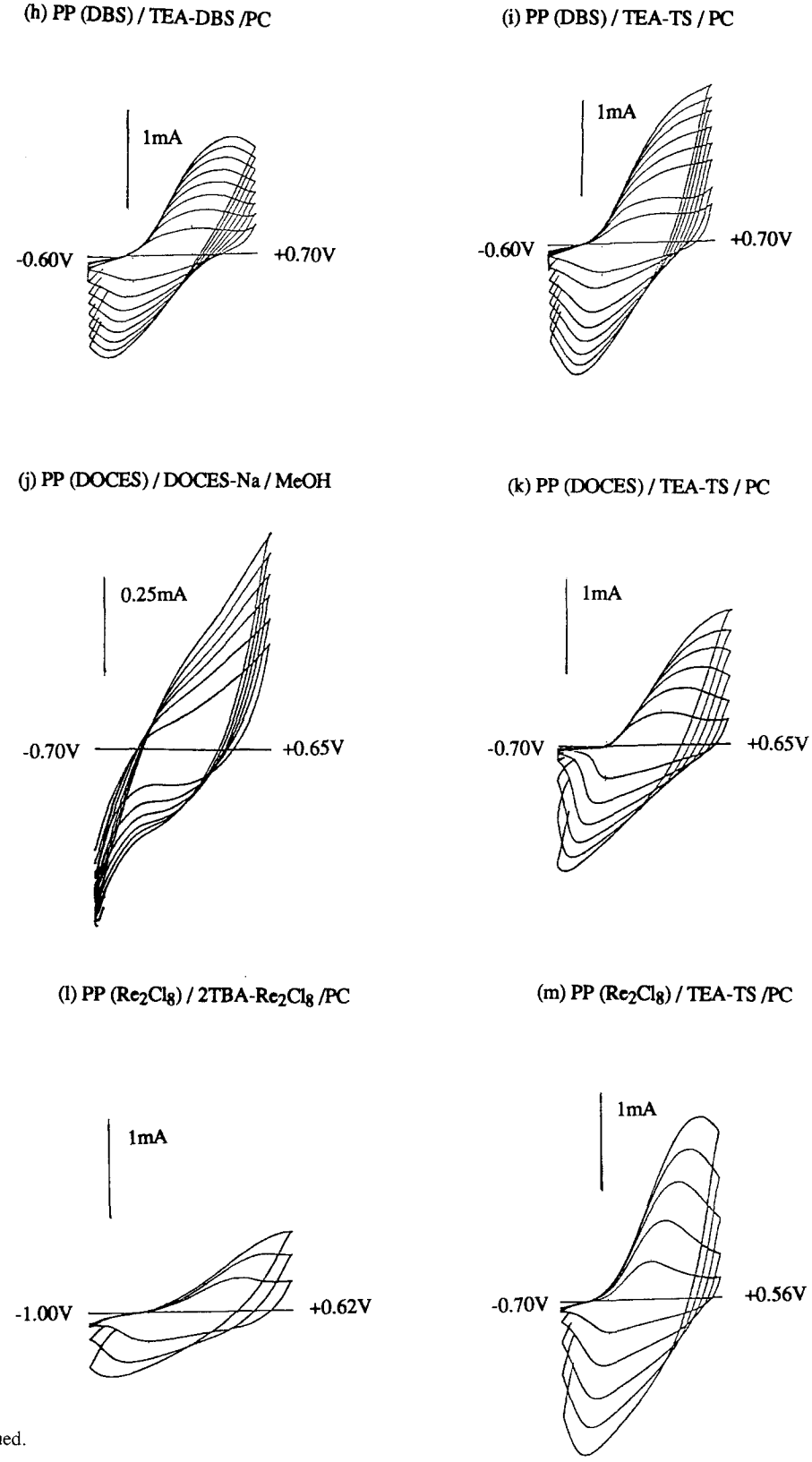

Figure 11 Continued.

In one experiment, the PPy/PTSA was cycled from -0.80 to $+0.3$ V in a clean TEA-TS/PC solution for 1530 times in open air. The film did not show any signs of degradation and the cyclic voltammogram of the film did not change (Fig. 14a). In the case of PPy/TS where it was cycled from -1.10 to $+0.80$ V under the same conditions 1500 times, the CV was flattened (Fig. 14b). This demonstrates that PPy/PTSA is more stable and less vulnerable to degradation than PPy/TS.

Graphs of i_p^a against square root of scan speed ($v^{1/2}$) and i_p^a against v for polypyrrole with different anions incorporated, in TEA-TS/PC and TEA-X/PC systems were plotted, see Fig. 15. The i_p^a against $v^{1/2}$ plots are straight lines in all cases but they do not pass through the origin. This indicates that the oxidation of all polypyrrole films studied is not a simple diffusion-controlled process.

It can be imagined that when the neutral PPy film is being oxidized, the anions are adsorbed on the exter-

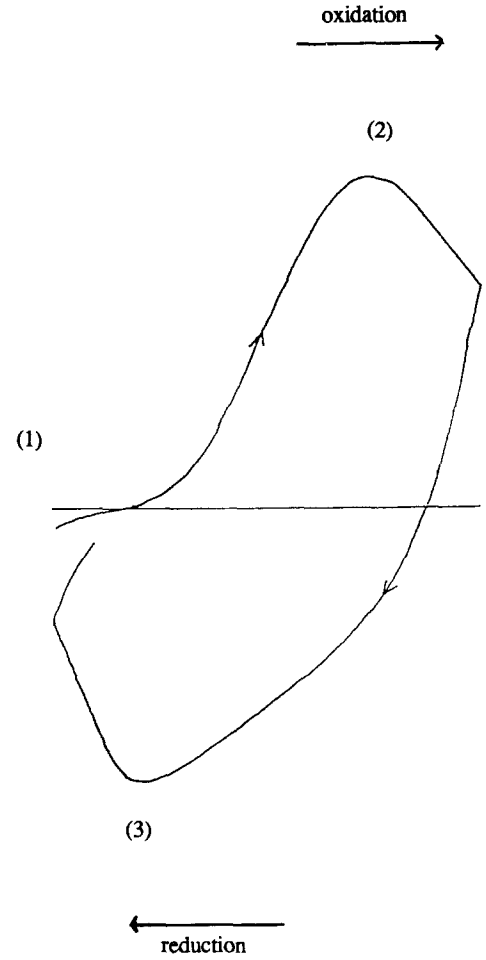

Figure 12 CV of a polypyrrole film.

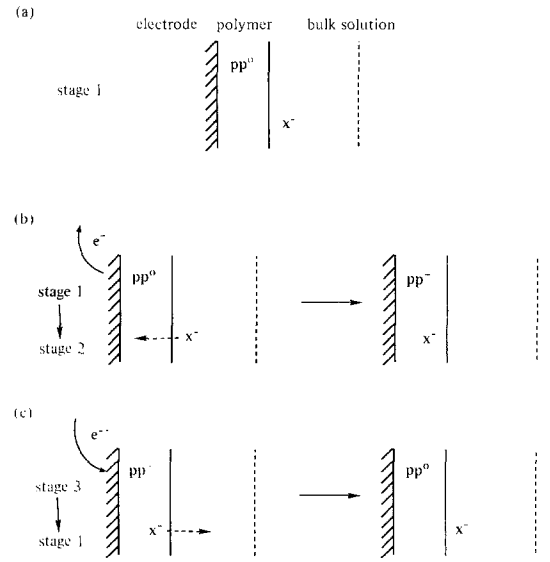

Figure 13 The transport of the anions during the redox reaction of a PP film.

nal and internal surfaces of the film first before entering the solid polymer. This depletion of the anions cause a diffusion gradient in the bulk solution. Also, the anions will diffuse into the matrix of the polymer due to the positive charges of the oxidized polymers, causing another diffusion gradient inside the film (Fig. 16). Therefore, the whole oxidation and anion transport process is not a simple single-step diffusion-controlled reaction.

2.9. Elemental analysis

Elemental analysis of various PPy films are given in Table III. Both PPy/TS, PPy/RE_2Cl_8 produced element proportions which closely met the required formula of $C_4H_3N_1(X)_n$, where X is the incorporated anion and n is the value of incorporation. This suggests that the electropolymerization mechanism of pyrrole in 2TBA-Re_2Cl_8/PC is less complex (in the sense that less organic species are involved in the solution) than those in which other large organic anion electrolytes are employed.

The carbon and hydrogen contents of PPy/DBS and PPy/DOCES are less than the required formula, which implies that they are more vulnerable to oxidation by air to form carbonyl structures in the backbone chain and also that the electropolymerization was more complicated. In Table III, we can see the pyrrole/anion ratios are very variable. In the case of PPy/PTSA, one $PTSA^{4-}$ ion was incorporated with fourteen pyrrole units. Since $PTSA^{4-}$ bears four negative charges, there is one positive charge localised among about 3.6 pyrrole units; this is close to the PPy/TS and PPy/DBS ratios. In the case of PPy/DOCES and PPy/PSA, the pyrrole/anion ratios are ten and unity respectively.

The above results suggest that the spatial arrangement of these anions in the matrix of the polymer films must be very different from each other. This may also have direct implications for the effective conjugation length and degree of branching and crosslinking for the different polymers.

TABLE II The peak current ratios (i_p^a/i_p^c) of PPy films with different anions incorporated

Counter-ion incorporated in PPy / electrolyte (solvent) in which PPy CV was taken	Peak current ratio i_p^a/i_p^c
TS/TEA-TS (PC)	0.89
PSA/TEA-PSA (PC)	1.20
PSA/TEA-TS (PC)	1.10
PSA*/TEA-PSA (PC)	1.20
PSA*/TEA-TS (PC)	1.08
PTSA/$LiClO_4$ (H_2O)	0.86
PTSA/TEA-TS (PC)	1.00
DBS/TEA-DBS (PC)	1.10
DBS/TEA-TS (PC)	1.00
DOCES/Na-DOCES (MeOH)	–
DOCES/TEA-TS (PC)	1.08
Re_2Cl_8/2TBA$^+$ $Re_2Cl_8^=$ (PC)	1.17
Re_2Cl_8/TEA-TS (PC)	1.23

*The PPy was prepared in the presence of 1% H_2O.

2.10. Optical absorption spectra

Thin polypyrrole films with different anions incorporated were prepared galvanostatically in 0.1 M TEA-X/ PC, on a platinum coated quartz glass (1.5 × 0.5 cm^2), where X was the corresponding anion. The current density was 0.3 mA cm^{-2} and the duration of polymerization was 3 min. All the films are black in colour. The optical absorption of the reduced films were measured, the films being reduced galvanostatically at the same current density in 0.1 M $LiClO_4$/

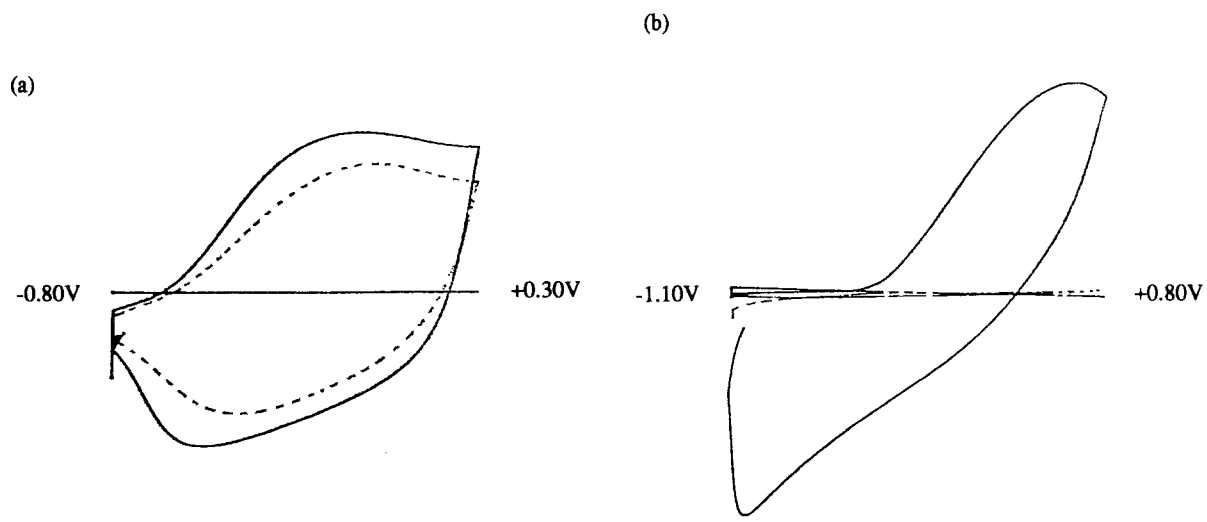

Figure 14 (a) CV of PPy/PTSA in 0.1 M TEA-TS/PC (against SCE); scan speed = 50 mV sec^{-1}; from −0.8 to +0.3 V. (——), after 1 cycle; (— —), after 1530 cycles. (b) CV of PP_y/TS in 0.1 M TEA-TS/PC (against SCE); scan speed = 50 mV sec^{-1}; from −1.10 to +0.8 V. (——), after 1 cycle; (— —), after 1500 cycles.

THF, with a silver wire as the counter electrode. All the redox reactions of the polymer films were carried out in a standard absorption cell in 0.1 M $LiClO_4$/THF, while the spectra were being recorded.

Figure 17 shows that the optical absorption spectra of all the films are similar. The strong absorption band of the oxidized polymer appears in the range 2.56–2.74 eV. The absorption bands of the intermediate partially reduced polymer appears at about 3.20 eV and 2.00 eV. The absorption band of the completely reduced polymer appears at about 3.20 eV.

During the doping process, the two states appearing in the gap between conduction and valence bands result from a depression of the LUMO and elevation of the HOMO. This is equivalent to bringing the π and π^* molecular orbitals closer by adding conjugated double bonds to the system. For the bipolaron (dication), the shift of the LUMO and the HOMO is larger than that for the polaron (cation radical) [48]. This is because in the bipolaron state, the polypyrrole has a conjugated structure including units of quinoid type (Fig. 18) in which the charge carriers are more delocalised than in the polaron state.

For the polaron state, there are 3 allowed optical transitions whereas there are 2 in the bipolaron state and 1 in the neutral state (Fig. 19). The 3.2 eV absorption in the neutral polypyrrole is the $\pi \rightarrow \pi^*$ (interband) transition. At intermediate doping levels this remains and a second weaker band appears at 2.0 eV. In general the absorption is still rising at 1.5 eV the lower limit of the spectral range investigated. Since transition 2 of Figs. 19b and c lies well outside the accessible range, this suggests that polarons (radical cations) are the predominant species under these conditions. At higher oxidation levels the interband transition is lost, except weakly in PPy/DBS. Bands are observed at 2.8 eV and just outside the experimental range, i.e. between 1.0 and 1.5 eV. These fit with the bipolaron (dication) band structure shown in Fig. 19d. These results are in agreement with spectra reported in the literature and calculation of the energy levels of polypyrrole [49, 50]. The absorption maxima of polypyrrole films with different anions are listed in Table IV. This result suggests that anions incorporated into the PPy films do not affect the transition pattern during the redox reaction on the backbone structure. Furthermore they show that generally the oxidised PPy occurs in a bipolaron state; when it is partially reduced, the polaron state is obtained and in intermediate states mixtures of bipolaron and polaron states occur.

The anions did not contribute to the optical absorp-

TABLE III Elemental analyses of polypyrroles with different anions incorporated

PPy/ anions	C	H	N	S	O*	Cl	Re	Formula	Total composition	Pyrrole/anion ratio
PPy/TS	58.84	4.63	10.35	8.06	15.17	–	–	$C_{4.29}H_{3.92}N_{1.00}(TS)_{0.34}$	97.05	2.94
PPy/PSA	62.36	3.95		3.60	7.80	16.82	–	$C_{5.20}H_{6.87}N_{1.00}(PSA)_{0.93}$	94.53	1.08
PPy/PTSA	47.55	3.69	9.97	6.48	–	–	–	$C_{4.43}H_{4.76}N_{1.00}(PTSA)_{0.07}$	–	14.29
PPy/DBS	58.82	5.94	8.12	4.93	10.87	–	–	$C_{3.65}H_{2.49}N_{1.00}(DBS)_{0.27}$	88.68	3.70
PPy/DOCES	58.56	5.05	11.20	2.90	17.31	–	–	$C_{3.37}H_{1.23}N_{1.00}(DOCES)_{0.11}$	95.02	9.09
PPy/Re_2Cl_8	35.21	2.65	9.98	–	–	14.86	20.32	$C_{4.12}H_{3.72}N_{1.00}(Re_2Cl_8)_{0.078}$	83.02	12.82

PPy–polypyrrole
TS–toluenesulphonate
PSA–pyrenesulphonate
PTSA–pyrene-tetra-sulphonate
DBS–p-dodecylbenzene-sulphonate
DOCES–1,2-bis(decyloxycarbonyl)ethane-1-sulphonate
Re_2Cl_8–octachloro-dirhenate
*Direct measurements

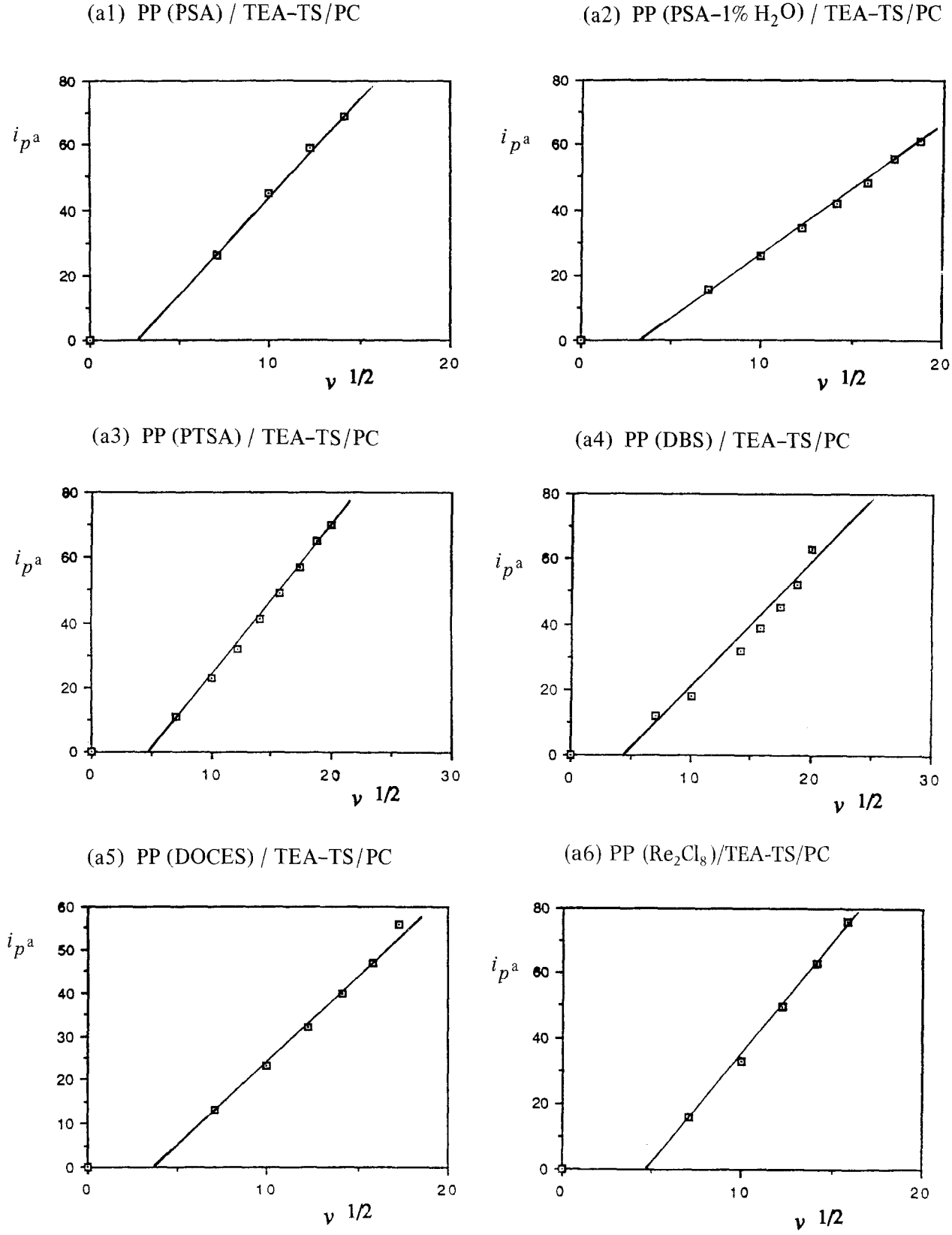

Figure 15 Graphs of (a) i_p^a against $v^{1/2}$ and (b) i_p^a against v plotted from the CVs of PP_y with different anions in different supporting electrolyte systems, namely, tetraethylammonium toluenesulphonate (TEA-TS) and the corresponding tetraethylammonium salts (TEA-X).

tion spectra except in the case of PPy/PSA. There are two sharp peaks at about 330 and 350 nm which are due to the optical absorption of the pyrene ring. The UV spectrum of PPy/PTSA was not recorded.

2.11 Raman spectroscopy

Thin PPy films with different anions similar to those used in the absorption experiments were prepared galvanostatically in ca. 0.1 M TEA^+X^-/PC, on a platinum coated quartz glass in open air. The details of the technique was reported previously [11].

The Raman spectra of the oxidised PPy films with different anions are similar to each other (Fig. 20). The assignments of the peaks is shown in Table V. These assignments were made on the basis of comparisons with the spectra of substituted pyrrole monomer [51] and deuterated PPy films [52, 53]. The bands with the highest intensity at 1573–1587 cm^{-1} are assigned to

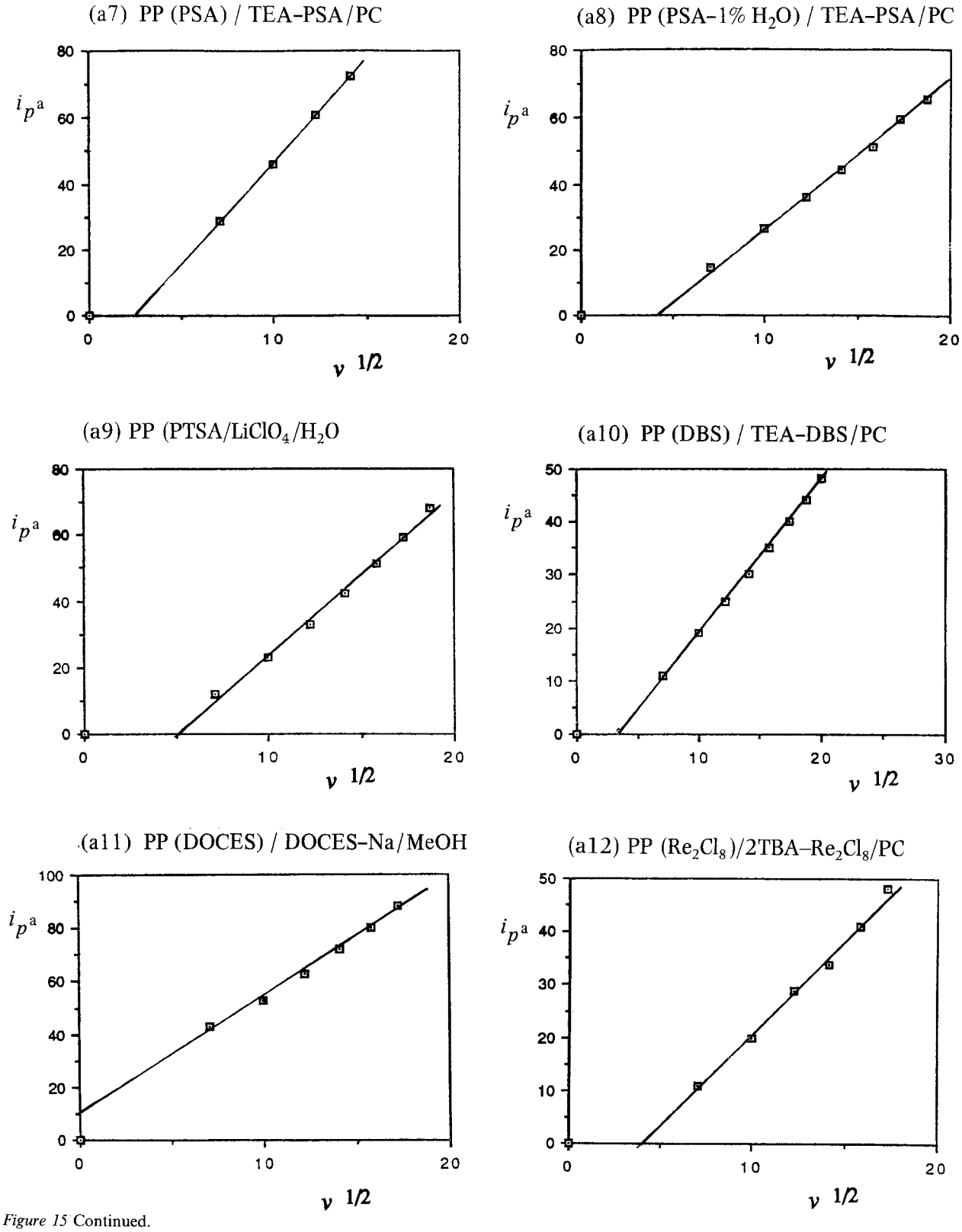

Figure 15 Continued.

TABLE IV Optical absorption spectra data of polypyrrole with different anions incorporated

Polymer/counter-ion	Peak at oxidized state	Peaks at the intermediate reduced state		Peak at the completely[§] reduced state
PPy/TS	452 nm (2.74 eV)	640 nm (1.94 eV)	440 nm (2.80 eV)[‡]	418 nm (2.96 eV)
PPy/PSA	468 nm (2.65 eV)	608 nm (2.04 eV)	384 nm (3.23 eV)*	384 nm (3.23 eV)
PPy/PTSA	–	–	–	–
PPy/DBS	484 nm (2.56 eV)	568 nm (2.18 eV)	384 nm (3.23 eV)*	384 nm (3.23 eV)
PPy/DOCES	468 nm (2.65 eV)	596 nm (2.08 eV)	396 nm (3.13 eV)*	396 nm (3.13 eV)
PPy/Re_2Cl_8	456 nm (2.74 eV)	616 nm (2.02 eV)	424 nm (2.92 eV)[†]	424 nm (2.92 eV)

*Reduction for 30 sec.
[†] Reduction for 120 sec.
[‡] Reduction for 150 sec.
[§] Reduction for 5 to 10 min.

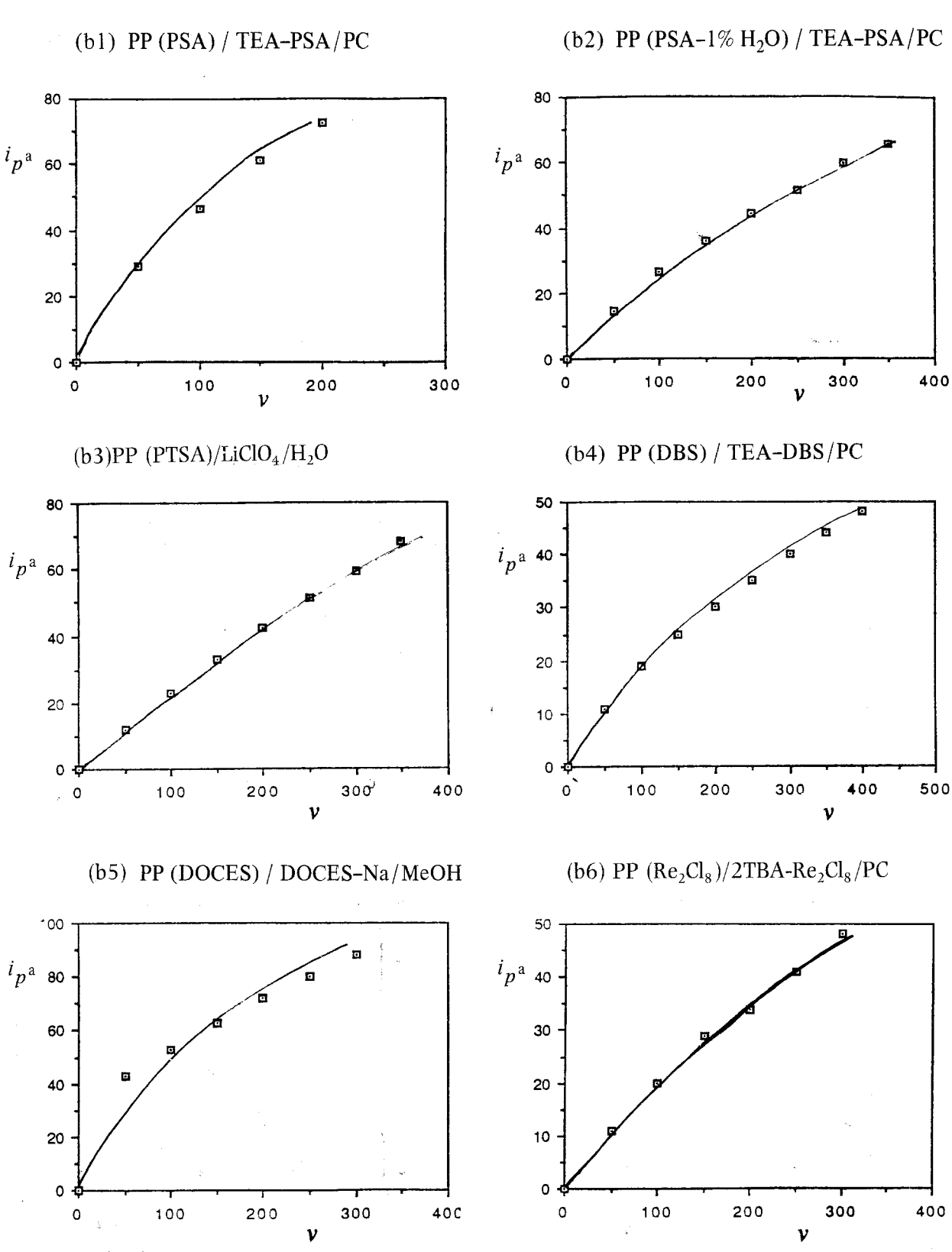

Figure 15 Continued.

the backbone C=C stretching of those oxidised PPy films. It can be seen that PPy/Re_2Cl_8 has the lowest backbone stretching frequency (1573 cm^{-1}) next to PPy/TS (1570 cm^{-1}) whereas PPy/PSA has the highest (1587 cm^{-1}). This suggests that the PPy/Re_2Cl_8 and PPy/TS have a higher degree of chain conjugation backbone with less branching than the other systems. This was also supported by the results in Table I, where it was shown that the redox potential of PPy/Re_2Cl_8 is lower than that of PPy/PSA. This stands in contrast to the very low pyrrole/anion ratio found from elemental analysis in which a fully quinoidic chain would be expected if DOCES phase separation did not occur. In this case the Raman result could imply a very high degree of chain disorder with very short conjugation lengths.

In the Raman investigation of PPy/Re_2Cl_8, the spectrum was scanned from 100 to 2000 cm^{-1}. Due to the heavy fluourescence effect and the low laser power (3 mW) used, the $\delta \rightarrow \delta^*$ transition of $Re_2Cl_8^{2-}$ was

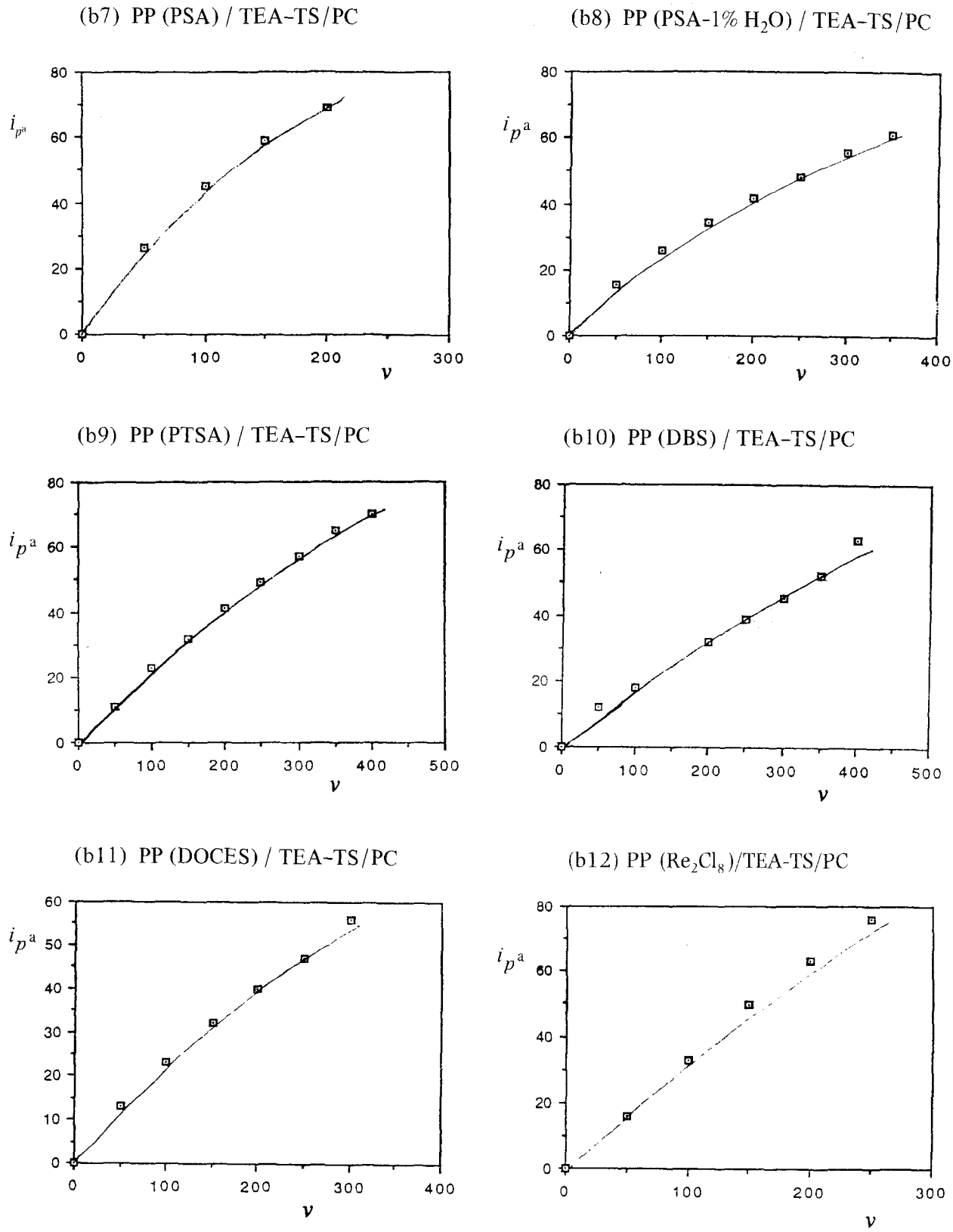

Figure 15 Continued.

not detected in the area about 275 cm^{-1} [54] and neither could the $\delta \rightarrow \delta^*$ transition of the dimeric ion be detected.

2.12. Atom bombardment (FAB) and thermal stability

Free-standing polypyrrole samples were used for all FAB experiments. The bombardments were on the electrode facing surfaces of the films. This technique was employed to investigate the structure and the approximate chain length of the polymer. The FAB results are shown in Fig. 21. Not many fragment peaks were obtained. There is a common molecular ion peak $(M + 1)^+$ at 133 which is equivalent to the molecular mass of the pyrrole dimer. In the cases of PPy/PSA, PPy/PSTA, PPy/Re_2Cl_8 and PPy/DOCES, the highest molecular mass peak detected is 392 corresponding to the pyrrole hexamer. The trimer is also found in the case of PPy/Re_2Cl_8. This suggests that the building units for polypyrrole would be mainly dimers, some

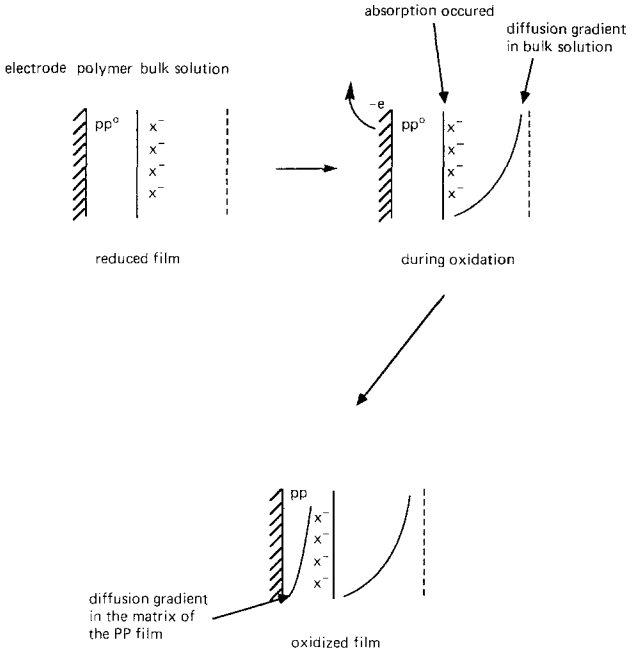

Figure 16 The diffusion of anions during the oxidation of a PPy film.

trimers and hexamers. Surprisingly, none of the fragment peaks of those anions could be deduced from the spectra except Re and Cl_8.

Preliminary results on the relative thermal stabilities of the materials in a nitrogen atmosphere are shown in Fig. 22. In all cases a low temperature weight loss occurs from room temperature up to about 180° C. This is due to solvent volatilization and DSC observations confirm that the peak temperatures for this process extend from 74° C for PPy/DOCES to 115° C for PPy/TS. In most cases the weight loss behaviour above 200° C can be accounted for by anion loss in a single stage, such as for TS^- and $PTSA^{4-}$, or at least two stages in the cases of DBS^- and $DOCES^-$. In the latter case loss of benzenesulphonate or ester sulphonate groups are considered to precede alkane chain decomposition. In contrast the behaviour of PPy/PSA and PPy/Re_2Cl_8 suggests that anion loss may be proceeded by more significant PPy breakdown above 600° C. These results suggest that PPy/TS and PPy/PTSA are the most thermally stable systems of the group.

2.13. Electrical conductivity

The conductivities of the polymers were measured by a four-probe technique, the current being supplied by a Farnell L30DT stabilised power supply and the voltage measured with a multimeter. Four leads are attached to the polymer in the square van der Pauw arrangement [55] using silver paste. A current (I) is passed between two adjacent contacts and the voltage drop (V) across the other two is measured. The conductivity σ is given by

$$\sigma = \frac{\ln 2}{\pi d} \frac{I}{V} \quad (1)$$

where d is the thickness of the sample, which is much less than the spacing between the probes. The measurements were made in open air at room temperature, and conductivities in the range of 1×10^{-3} to 50 S cm^{-1} (Table VI) were obtained.

In the previous CV and Raman sections. We predicted that the larger the anion incorporated in the PPy film, the higher the degree of conjugation in the backbone. Hence, higher conductivity could be expected. But from Table VI, this is not the case. The conductivity of PPy/TS is the highest, whereas the conductivities of PPy/Re_2Cl_8 and PPy/PTSA are medium, PPy/PSA and PPy/DBS the lowest.

This can be explained since the main factors limiting the conductivity are the carrier mobility, and the carrier concentration. The effective carrier mobility depends on at least three elements. They are (1) intramolecular transport which is concerned with the carrier moving along the conjugated backbone (Fig. 23 process A); (2) intermolecular transport which is concerned with the carrier hopping from one backbone to the other (Fig. 23 process B) and (3) interparticle transport (Fig. 23 process C) plays a major role in limiting the conductivity in those materials. Whilst PPy/DBS and PPy/PSA have different anion sizes and degrees of chain perfections, they both have open morphologies and exhibit the lowest conductivities. In contrast and PPy/TS and PPy/PTSA contain very small and very large anions respectively but both are densely packed and exhibit much higher conductivities; PPy/TS being the most densely packed has the highest value. Similar effects have been observed in other systems with bulky substitutions [21].

The exception to this is PPy/Re_2Cl_3 which has a very open morphology but a conductivity comparable to PPy/PTSA. In this case the pyrrole/anion-charge ratio is only 6 in comparison with 3 for the higher

TABLE V Raman peak frequencies of oxidized polypyrrole incorporated with different anions and their peak assignments

Peak frequencies (cm^{-1}) of polypyrrole with						Peak assignments
TS	PSA	PTSA	DBS	Re_2Cl_8	DOCES	
1573	1587	1579	1579	1573	1579	C=C backbone stretching
1483	1496	1485	1482	1464	1480	Ring stretching
1381	1400	1410	1400	–	1405	Ring stretching
1323	1365	1365	1323	1357	1360	Ring stretching
–	1280	1307	–	–	1307	Ring stretching
1243	1227	1235	1256	1232	1261	Ring streching
–	–	1200	–	–	–	–
–	1072	1077	–	–	1083	C–H bending
1053	1040	1050	1050	1045	1045	N–H in-plane deformation
971	957	968	973	965	968	C–H in-plane deformation
925	920	925	925	925	925	C–H out-of-plane deformation

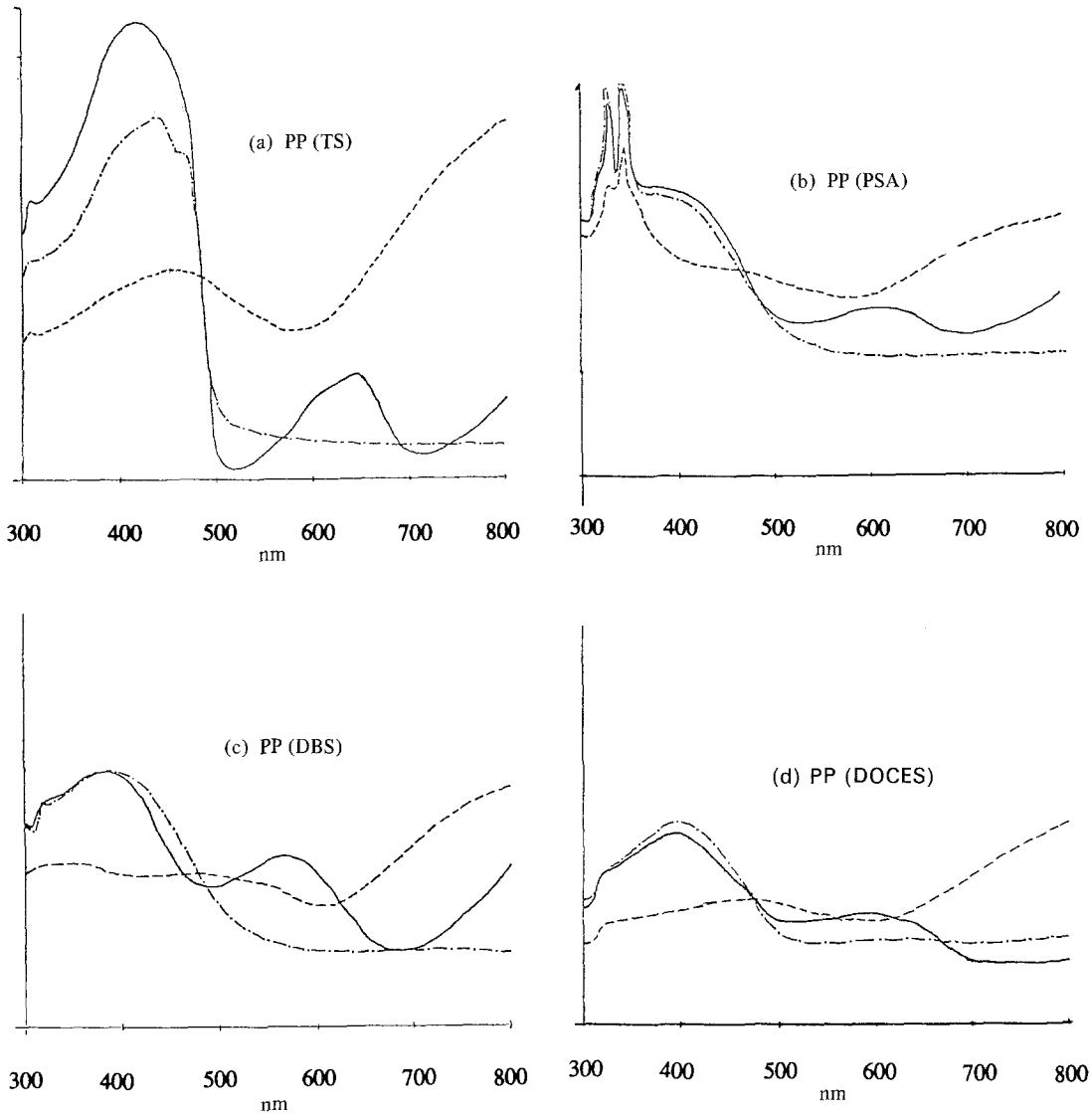

Figure 17 The optical absorption spectra of oxidized and reduced PPy films with (a) TS, (b) PSA, (c) DBS, (d) DOCES and (e) Re_2Cl_8 anion.

conductivity material but it exhibits some superlattice characteristics and this could favour higher intra- and inter-molecular mobility.

3. Conclusions

We have studied the chemical and physical properties of pyrrole polymers containing counterions that differ markedly from one another. While some properties of the polymer films are strongly influenced by the choice of counterions, others are hardly affected. Thus while morphology and the degree of order show wide variations as shown by SEM, Raman spectra and X-ray diffraction, the electronic excited states, seen in the optical spectra, are all very similar. Though the anions used might be expected to affect charge carriers by providing alternative sites for hopping conductivity, the only influence detected was on the separation of the polymer chains. Thus we can conclude that the electronic properties are determined by the polymeric cation network. The structure of this network is determined by the overall arrangement of polymer chains and counterions. These structural changes have little

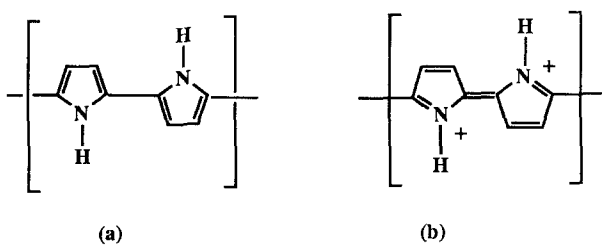

Figure 18 The (a) non-conjugated aromatic units and (b) conjugated quinoid units of polypyrrole.

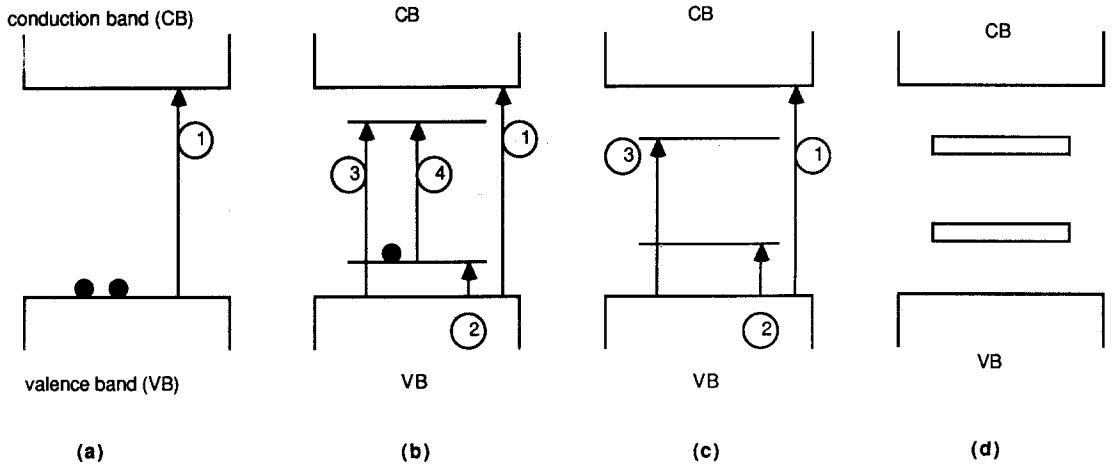

Figure 19 Schematic molecular levels of (a) neutral polypyrrole, (b), (c) lightly doped polymer for (b) positive polarons and (c) positive bipolarons, (d) heavily doped polypyrrole with bipolaron bands.

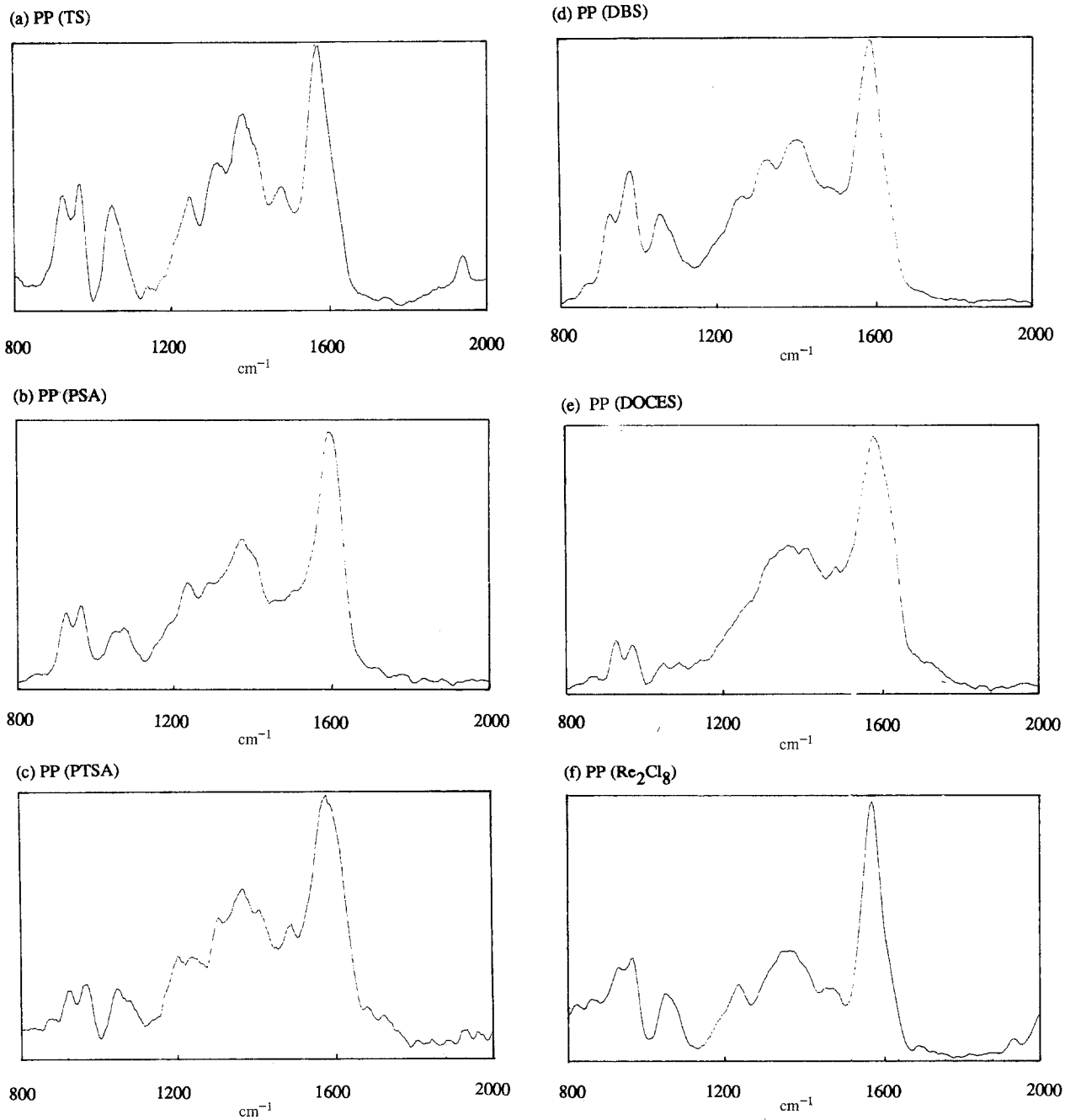

Figure 20 Raman spectra of PPy with different anions incorporated, (a) PPy/TS, (b) PPy/PSA, (c) PPy/PTSA, (d) PPy/DBS, (e) PPy/DOCES and (f) PPy/Re_2Cl_8.

TABLE VI Physical form and conductivities of polypyrrole films with different anions incorporated

PPy/anion	Nature of product	Conductivity ($S\,cm^{-1}$)
PPy/TS	Strong, dense, flexible, fully dense structure	48.5
PPy/PSA*	Powdery, brittle, open structure	2.60×10^{-3}
PPy/PTSA	Brittle, inflexible, dense structure but voided	2.10
PPy/DBS	Strong, flexible, open structure	6.40×10^{-3}
PPy/DOCES	Brittle, thin, layer forms, dense but voided	–
PPy/Re_2Cl_8	Strong, soft, highly flexible, open structure	5.00

*Compressed disc.
–Too brittle to form even a compressed disc.

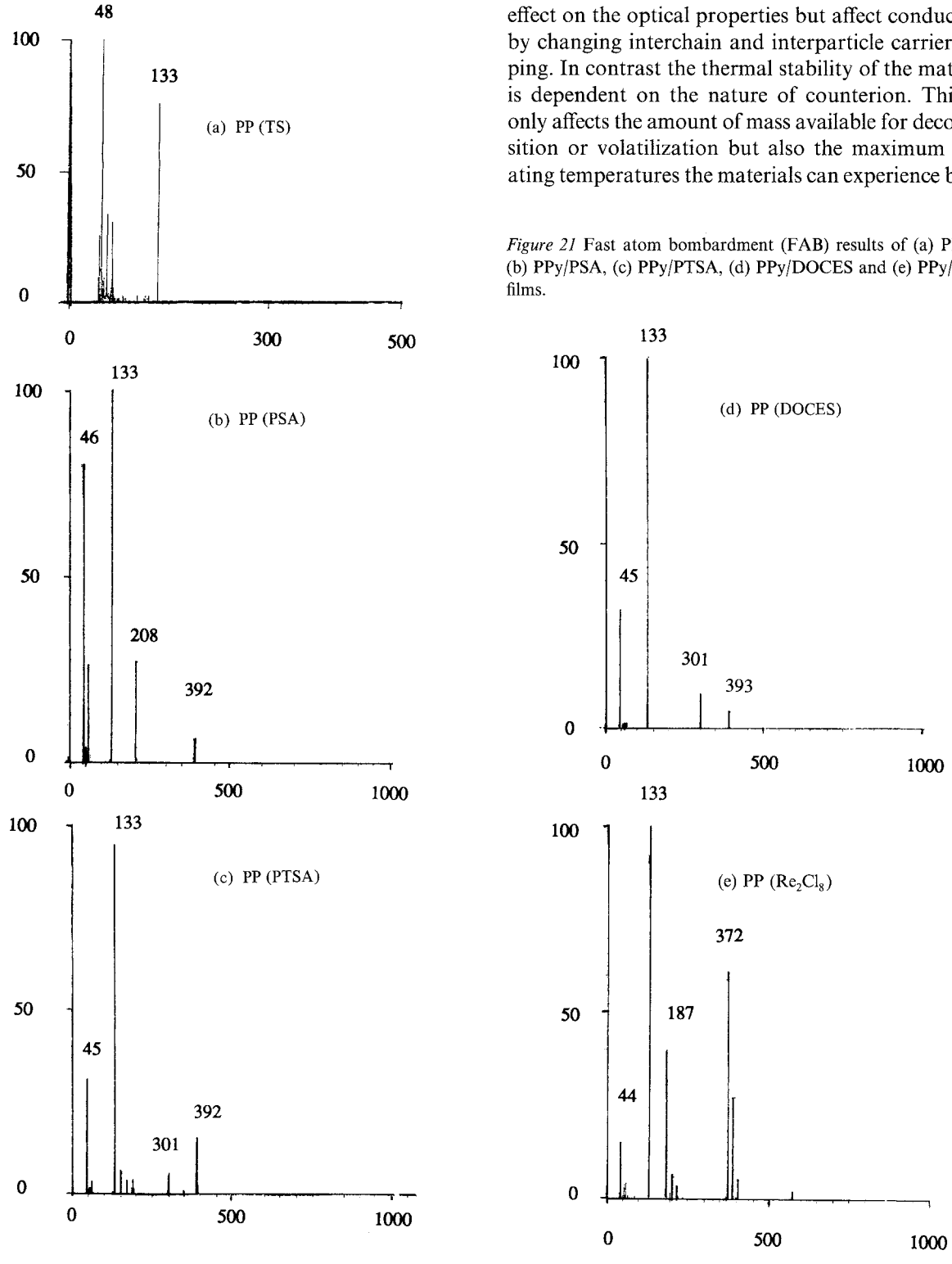

Figure 21 Fast atom bombardment (FAB) results of (a) PPy/TS, (b) PPy/PSA, (c) PPy/PTSA, (d) PPy/DOCES and (e) PPy/Re_2Cl_8 films.

effect on the optical properties but affect conductivity by changing interchain and interparticle carrier hopping. In contrast the thermal stability of the materials is dependent on the nature of counterion. This not only affects the amount of mass available for decomposition or volatilization but also the maximum operating temperatures the materials can experience before

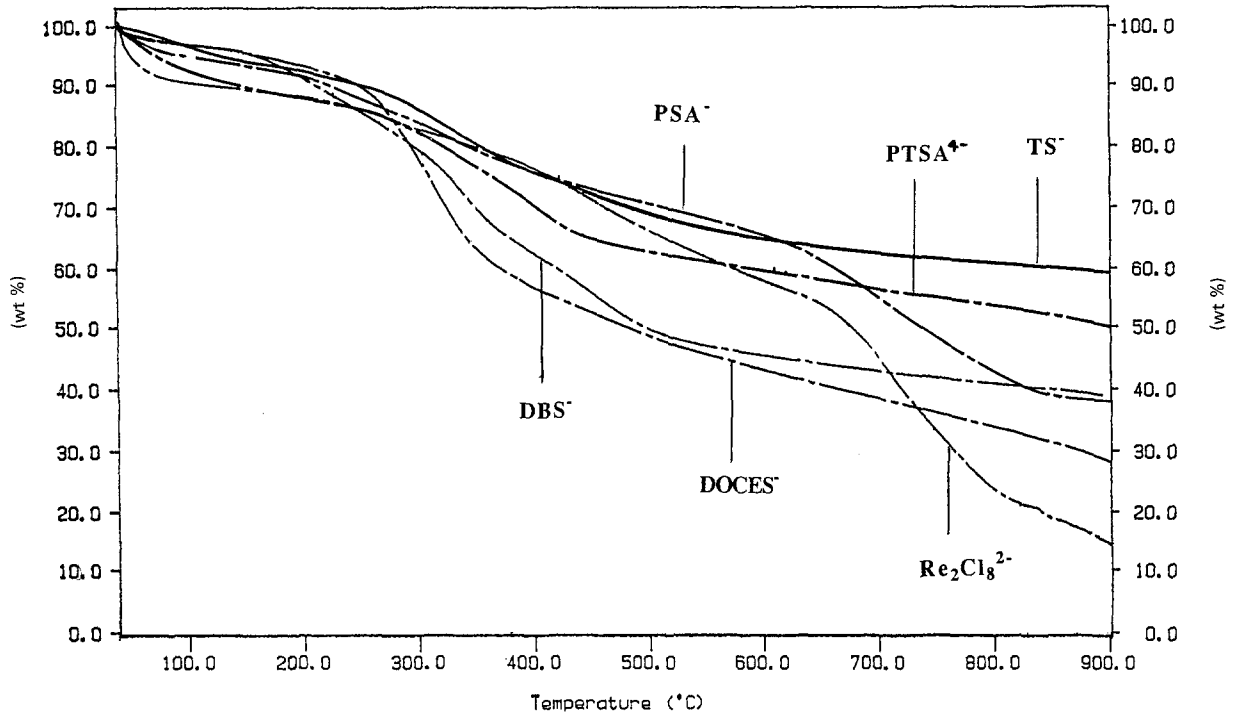

Figure 22 Thermogravimetric analysis of different polypyrrole films in a nitrogen atmosphere at a heating rate of 5° C min^{-1}.

counterions are lost. Similarly, morphology would have a significant influence on mechanical deformation and strength but the counterions are likely to control flexibility and fracture toughness.

There are also a number of common features in the electrochemistry of these systems. In most cases the redox potentials of the polymer can be related to the size of the counterion through its influence on chain structure and packing during electropolymerization. Similarly the counterion-charge to pyrrole stoichiometry generally corresponds to one positive charge to every three polymer repeat units, even in the case of the $PTSA^{4-}$ anion. However, there are some unusual stoichiometries for the PSA^-, $DOCES^-$ and $Re_2Cl_8^{2-}$ anions which may have special significance. $Re_2Cl_8^{2-}$ is particularly interesting because in spite of its lower stoichiometry and very open morphology it has a relative high conductivity and evidence exists for a superlattice. Unfortunately in the case of TPB the reaction of the counterion inhibits the electropolymerization of pyrrole.

These results illustrate that the physical properties and electrochemical behaviour of polypyrrole strongly depends on the nature of the counterion and its affect on chain perfection and packing and bulk morphology. Whilst some general trends have been found much of the detail remains to be understood.

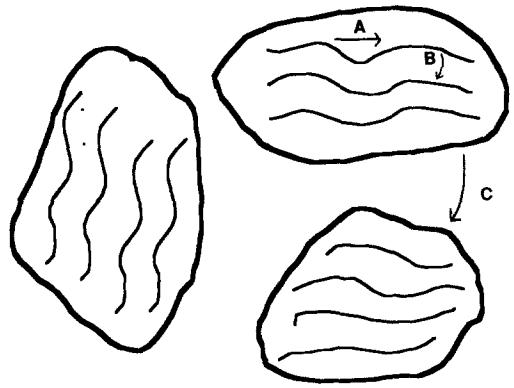

Figure 23 Conductivity network of a conducting polymer. (A) indicates an intramolecular transport, (B) indicates an intermolecular transport, (C) indicates an interparticle transport of charge carriers.

References

1. K. KANETO, M. MAXFIELD, D. P NAIRNS, A. G. MACDIARMID, and A. J. HEEGER, *J. Chem. Soc., Faraday Trans.* **78** (1982) 3417.
2. M. JOSOWICZ and J. JANATA *Anal. Chem.* **58** (1986) 514.
3. P. BURGMAYER and R. W. MURRAY, *J. Electroanal Chem.* **147** (1983) 339.
4. H. YONEYAMA, K. WAKAMOTO and H. J. TAMURA, *Electrochem. Soc.* **132** (1985) 241K.
5. J. W. THACKERAY, H. S. WHITE and M. S. WRIGHTON *J. Phys. Chem.* **89** (1985) 5133.
6. C. K. CHIANG, C. R. FINCHER Jnr, Y. W. TARK, A. J. HEEGER, H. SHIRAKAWA, E. J. LOUIS, S. C. GAU, and A. G. MACDIARMID, *Phys. Rev. lett.* **39** (1977) 1098.
7. A. F. DIAZ, and K. K. KANAZAWA, *J. Chem. Soc., Chem. Commun.* (1979) 635.
8. M. SATOH, K. KANETO and K. YOSHIMA, *Syn. Met.*, **14** (1986) 289.
9. M. OGASAWARA, K. FUNAHASHI, T. DEMURA, T. HAGIWARA, and K. IWATA, *ibid.* **14** (1986) 61.
10. G. K. CHANDLER, and D. PLETCHER, *Chem. Soc. Spec. Period. Rep. Electrochem.* **10** (1985) 117.
11. K. M. CHEUNG, D. BLOOR, and G. C. STEVENS, *Polymer* **29** (1988) 1709.
12. J. P. I. LUNDSTROM, and T. SKOTHEIM, *J. Electrochem. Soc.* **129** (1982) 1685.
13. J. RUHE, T. A. EZQUERRA and G. WEGNER, *Syn. Met.*, **28** (1989) C177.
14. C. E. LOADER, and H. J. ANDERSON, *Tetrahedron*, **25** (1969) 3879.
15. J. K. GROVES, N. E. CUNDASAURNY, and H. J. ANDERSON, *Can. J. Chem.* **51** (1973) 1089.
16. R. M. ACHESON, and J. M. VERNON *J. Chem. Soc.* (1961) 457.
17. M. K. A. KHAN, K. J. MORGAN and D. P MORREY, *Tetrahedron* **22** (1966) 2095.

18. M. R. BRYCE, A. CHISSEL, P. KATHIRGAMANATHAN, D. PARKER and R. M. N. SMITH, *J. Chem. Soc., Chem. Commun.* (1987) 466.
19. D. O. CHENG, T. L. BOWMAN and E. LEGOFF, *J. Heterocyclic Chem.* **13** (1976) 1145.
20. J. RUHE, T. A. EZQUERRA, M. MOHAMMADI, V. EUKELMANN, F. KREMER, and G. WEGNER, *Syn. Met.* **28** (1989) C217.
21. J. RUHE, C. KROHNKE, T. A. EZQUERRA, F. KREMER and G. WEGNER, *Ber. Bunsenges, Phys. Chem.* **91**(9) (1987) 885.
22. A. MOHAMMADI, M. A. HASAN, B. LIEDBERG, I. LUNDSTROM and W. R. SALANECK, *Syn. Met.* **14** (1986) 189.
23. A. MOHAMMADI, I. LUNDSTROM, W. R. SALANECK and O. INGANAS, *Chemtronics* **1** (1986) 171.
24. X. Q. YANG, T. INAGAKI, T. A. SKOTHEIM, Y. OKAMOTO, L. SAMUELSON, G. BLACKBURN and S. TRIPATHY, *Mol. Cryst. Liq. Cryst.* **160** (1988) 253.
25. A. K. M. RAHMAN, L. SAMUELSON, D. MINEHAN, S. CLOUGH and S. TRIPATHY, *Syn. Met.* **28** (1989) C237.
26. X. Q. YANG, J. CHEM, P. D. HALE, T. INAGAKI and T. A. SKOTHEIM, *ibid.* **28** (1989) C251.
27. K. HONG and M. F. RUBNER *Thin Solid Films* **160** (1988) 187.
28. K. G. NEOH, T. C. TAN and E. T. KANG, *Polymer* **29** (1988) 553.
29. T. H. CHAO, and J. MARCH *J. Polym. Sci., Part A* **26** (1988) 743.
30. S. RAPI, V. BOCCHI, and G. P. GARDINI, *Syn. Met.* **24** (1988) 217.
31. L. F. WARREN and D. P ANDERSON, *J. Electrochem. Soc.* **134** (1987) 101.
32. G. BIDAN, E. M. GENIES, and M. LAPKOWSKI, *J. Electroanal. Chem.* **251** (1988) 297.
33. G. BIDAN and M. LAPKOWSKI, *Syn. Met.* **28** (1989) C113.
34. S. TAKEO, O. AKIRA, A. MASAJI and H. KENICHI, *J. Chem. Soc. Faraday Trans. I* **84**(11) (1988) 3941.
35. D. T. GLATZHOFES, J. ULANSKI and G. WEGNER, *Polymer* **28** (1987) 449.
36. A. F. DIAZ and J. C. LACROIX, *New J. Chem.* **12** (1988) 171.
37. S. C. LARRY, C. K. GLENN, and J. P. WILLIAM, *J. Phys. Chem.* **92** (1988) 12.
38. F. M. MENGER, and L. G. WHITESELL, *J. Org. Chem.* **52** (1987) 3793.
39. K. TOYOKI and O. YOSHIO, *Bull. Chem. Soc. Jpn.* **51**(6) (1978) 1877.
40. M. G. KANATZIDIS, M. HUBBARD, L. M. TONGE and T. J. MARKS, *Syn. Met.* **28** (1989) C89.
41. M. G. KANATZIDIS, M. HUBBARD, L. M. TONGE and T. J. MARKS, *J. Amer. Chem. Soc.* **109** (1987) 3797.
42. L. MEITIES and P. ZUMAN, "Handbook series in Ong. Electrochemistry", Vol. 1, (CRC Press, Inc. 1976) p. 506.
43. J. FORRENT *J. Chem. Soc.* (1960) 574.
44. S. AEIYACH and P. C. LACAZE *J. Polym. Sci. Part A* **27** (1989) 515.
45. S. ASAVAPIRIYANOUT, G. K. CHANDLER, G. A. GUNAWASDENA and D. PLETCHER, *J. Electroanal. Chem.* **177** (1984) 229.
46. E. STECKHAN, "Topics in current chemistry 142 - Electrochemistry I", (Springer Verlag, 1987), Ch. 1.
47. T. SHONO, A. IKEDA, J. HAYASHI and S. HAKOZAKI, *J. Amer. Chem. Soc.* **97**(15) (1975) 4261.
48. J. L. BREDAS, J. C. SCOTT, K. YAKUSHI and G. B. STREET, *Phys. Rev.* **B30** (1984) 1023.
49. W. FORD, C. B. DUKE and W. R. SALANECK, *J. Chem. Phys.* **77** (1982) 5030.
50. J. L. BREDAS and G. B. STREET, *Acc. Chem. Res.* **18** (1985) 309.
51. F. R. DOLLISH, W. G. FATELEY and F. F. BENTLEY, "Characteristic Raman Frequencies of Organic Compounds", (Wiley, New York, 1974) Ch. 16, p. 217.
52. Y. FUJII, Y. FURUKAWA, H. TAKENCHI, and I HARADA, "*Proc. IXth Int. Conf. on Raman Spectroscopy, Tokyo*" (*IUPAC*, 1984) p. 412.
53. Y. FURUKAWA, S. TAZAWA, Y. FUJII and I. HARADA, *Syn. Met.* **24** (1988) 329.
54. J. H. C. ROBIN and J. S. MARTIN, *Inorg. Chem.* **22** (1983) 1214.
55. H. H. WIEDER, "Laboratory Notes on Electrical and Galvanomagnetic Measurements, Materials Science Monographs", Vol. 2 (Elsevier, Amsterdam, 1979) Ch. 1.

Received 13 June
and accepted 29 June 1989